Article

Nephroprotective Effects of Cardamonin on Renal Ischemia Reperfusion Injury/UUO-Induced Renal Fibrosis

Banghua Zhang,[||] Zhi-Yuan Chen,[||] Zhengyu Jiang, Shiyu Huang, Xiu-Heng Liu,* and Lei Wang*

Cite This: J. Agric. Food Chem. 2023, 71, 13284−13303

Read Online

ACCESS | 📊 Metrics & More | 📖 Article Recommendations | SI Supporting Information

ABSTRACT: Acute kidney injury and chronic renal fibrosis are intractable pathological processes to resolve, yet limited strategies are able to effectively address them. Cardamonin (CAD) is a flavonoid with talented antioxidant, anti-inflammatory capacity, and satisfactory biosafety. In our study, animal and cellular models of renal ischemia/reperfusion (I/R) and unilateral ureteral obstruction (UUO) were successfully constructed to confirm whether CAD confers protective effects and underlying mechanisms. Animal experiments demonstrated that CAD application (100 mg/kg) distinctly ameliorated tissue damage and improved renal function. Meanwhile, the continuous oral administration of CAD after UUO surgery efficiently inhibited renal fibrosis as confirmed by hematoxylin−eosin (H&E), Sirius red, and Masson staining as well as the downregulated mRNA and protein expression of collagen I, α-smooth muscle actin (α-SMA), collagen III, and fibronectin. Interestingly, in transforming growth factor β1 (TGF-β1)-stimulated and hypoxia/reoxygenation (H/R)-exposed human kidney-2 (HK-2) cells, protective effects of CAD were again authenticated. Meanwhile, we performed bioinformatics analysis and constructed the "ingredient−target−pathway−disease" network to conclude that the potential mechanisms of CAD protection may be through the regulation of oxidative stress, inflammation, apoptosis, and mitogen-activated protein kinase (MAPK) pathway. Furthermore, experimental data validated that CAD evidently decreased the reactive oxygen species (ROS) production and malondialdehyde (MDA) content while depressing the mRNA and protein expression of inflammatory markers (tumor necrosis factor-α (TNF-α), interleukin-6 (IL-6), and Il-1β) and inhibiting apoptosis as evidenced by decreased levels of P53, BAX, cleaved caspase-3, and apoptotic rate in renal I/R and UUO models. In addition, the impact of CAD on restraining oxidative stress and inflammation was attributed to its ability to elevate antioxidant enzyme activities including catalase, superoxide dismutase 1 (SOD1), and superoxide dismutase 2 (SOD2) and to inhibit the inflammation-associated MARK/nuclear factor-κB (MAPK/NF-κB) signaling pathway. In conclusion, cardamonin restored the antioxidative capacity to block oxidative stress and suppressed the MAPK/NF-κB signaling pathway to alleviate inflammatory response, thus mitigating I/R-generated acute kidney injury/UUO-induced renal fibrosis in vivo and in vitro, which indicated the potential therapeutic advantage of cardamonin in attenuating acute and chronic kidney injuries.

KEYWORDS: unilateral ureteral obstruction, renal ischemia/reperfusion injury, cardamonin, oxidative stress, inflammation, MAPK pathway

1. INTRODUCTION

Acute kidney injury (AKI) is one clinical syndrome in which kidney function deteriorates speedily over a quick period under harmful stimuli. Renal ischemia/reperfusion (I/R) injury has been testified to serve as one momentous factor leading to AKI.[1] The incidence of AKI is 10−15% in general patients and even up to 50% in intensive care units.[2] The mortality rate of patients with critical AKI is worrisome, and some patients are left with permanent renal decompensation or even progress to chronic kidney disease (CKD).[3] CKD is highly susceptible to progress into end-stage renal disease (ESRD), mainly due to complex pathophysiological activities and insufficient means of prevention and treatment.[4] As one public health problem, the prevalence of CKD is above 10% worldwide.[5] Therefore, persistently exploring strategies in preventing and treating AKI or CKD appears to be particularly worthwhile owing to their alarming morbidity and mortality.

Accumulating studies confirmed that oxidative stress as well as inflammation response is one of the primary molecular processes in renal I/R-generated AKI or renal fibrosis.[6] Renal fibrosis was characterized by myofibroblast expansion and extracellular matrix (ECM) deposition and is generally regarded as the dominating pathway for the CKD progression.[7] As an organ with abundant blood flow and distinguished oxygen consumption, the kidney performs its physiological functions such as renal tubular reabsorption through notable energy metabolism.[8] An imbalance in the oxidative/antioxidant system caused by pathological conditions will trigger the exaggerated formation of reactive oxygen species (ROS) and occurrence of oxidative stress, which not only harmfully devastated the cellular structure to perturb or interrupt normal physiological activities but also activated abnormal signaling pathways and induced inflammatory infiltration as well as renal cell death, eventually leading to
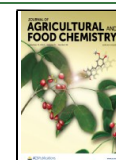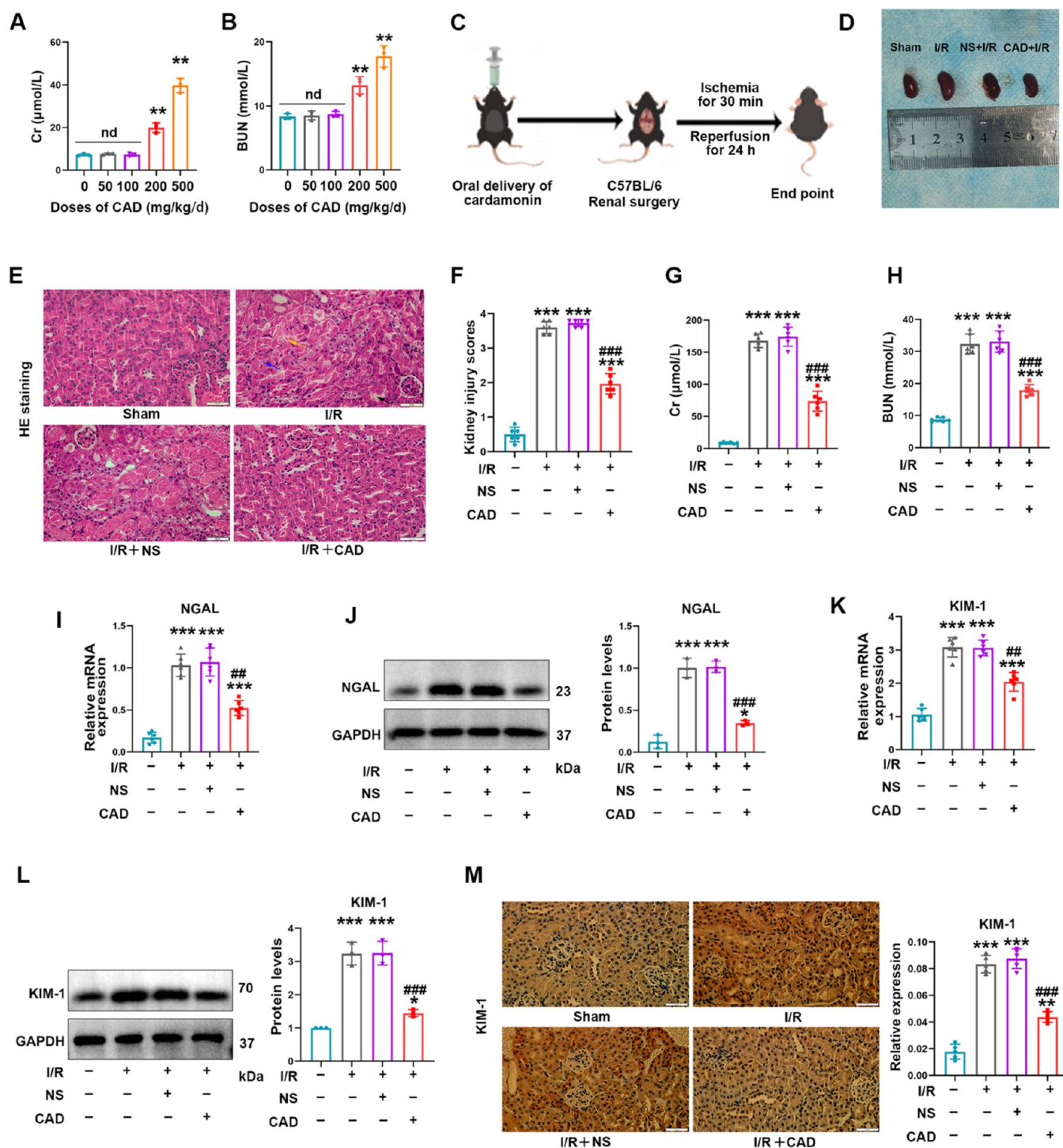
Figure 1. Cardamonin application remarkably alleviated acute kidney injury induced by renal I/R surgery in mice. (A, B) The impact of several doses of CAD on Cr and BUN in C57BL/6 mice. (C) Schematic diagram of CAD application in the renal I/R research model. (D) Typical images of the kidney shape and color in the I/R + CAD group and I/R + NS group. (E, F) H&E staining suggested that CAD administration effectively mitigated renal tissue injury including tubular dilatation (black arrow), brush border absence (yellow arrow), and tubular necrosis (purple arrow) during I/R surgery in mice (400×, scale bar = 50 μm). (G, H) Beneficial improvement of CAD on the renal function in mice undergoing I/R operation. (I) Relative mRNA expression and (J) protein levels of NGAL in all groups. (K, L) CAD employment obviously attenuated the high mRNA and protein expression of KIM-1 in the I/R group. (M) Immunohistochemical staining demonstrated the comparative expression of KIM-1 in four groups (400×, scale bar = 50 μm). Measurement data were expressed as mean ± SD, n = 6 per group. *P < 0.05, **P < 0.01, and ***P < 0.001 vs Sham. #P < 0.05, ##P < 0.01, and ###P < 0.001 vs I/R. n d, no statistical difference.

AKI.[9] Besides, oxidative stress could provoke multiple mechanisms to participate in glomerulosclerosis and tubulointerstitial fibrosis, contributing to renal fibrosis.[10] Accumulative research evidence authenticated that multiple kidney diseases

include complicated regulation between diverse inflammatory cells, abnormal initiation of cytokine release, and inflammatory infiltration.[11] Appropriate inflammation contributes to self-repair during the procedure of kidney injury, while persistent

and uncontrolled inflammatory response plays an influential part in the progression of AKI and renal fibrosis.[11,12] Consequently, antioxidative and anti-inflammatory agents are promising to be developed as candidates for alleviating acute kidney injury and renal fibrosis.

Cardamonin is known as one valued and representative member of the chalcone family and is derived from Alpinia katsumadai. Owing to its prominent inhibition properties in oxidative stress, tumorigenesis, inflammation, and infectious diseases, CAD is gradually revealing its potential to become a candidate strategy for therapeutics in related diseases.[13,14] For example, CAD protects against septic shock, osteoarthritis, and acute lung injury by obviously restraining the secretion of inflammatory cytokines and repressing inflammatory pathways.[15−17] Furthermore, the antioxidant pathways and capacities were enhanced after CAD treatment to successfully improve doxorubicin-generated cardiotoxicity, neurodegenerative disorders, and acute hepatic injury.[18−20] However, the beneficial influence and underlying molecular mechanisms of CAD on renal I/R-exposed AKI or unilateral ureteral obstruction (UUO)-caused CKD remain unexplored.

In this study, we innovatively investigated the valuable consequence of the gavage administration of CAD on C57BL/6 mice that underwent renal I/R or UUO surgery. Furthermore, Gene Ontology (GO) terms, Kyoto Encyclopedia of Genes and Genomes (KEGG) pathway enrichment analysis, and experiments verified that its positive role was through the decreased generation in oxidative stress and mitigated expression in inflammatory factors by activating antioxidant enzymes and hindering the mitogen-activated protein kinase/nuclear factor-κB (MAPK/NF-κB) signaling pathway. In HK-2 cells stimulated by H/R or transforming growth factor-β1 (TGF-β1), relevant findings are consistent with results from in vivo experiments. Our study presented CAD to become a possible therapeutic strategy in treating acute and chronic kidney disorders.

2. MATERIALS AND METHODS

2.1. Antibodies and Reagents. Cardamonin (HPLC ≥ 98%) was purchased from MedChemExpress (Shanghai, HY-N0279), and active recombinant mature TGF-β 1 protein was obtained from ABclonal (Wuhan, RP01458). Annexin V-FITC/PI apoptosis kit was supplied by Beyotime (Shanghai, C1062M). Poly(vinylidenedifluoride) (PVDF) membranes were bought from Millipore (Billerica, MA). The product source and product number of other kits are described accordingly below. According to the product instructions, dimethyl sulfoxide (DMSO) was used to dissolve CAD in vitro study, and the dissolution sequence of CAD in vivo experiments was as follows: 10% DMSO, 40% PEG300 (poly(ethylene glycol) 300), 5% Tween-80, 45% saline (solubility: ≥ 2.17 mg/mL).

2.2. Experimental Animals. Male C57BL/6 mice (20−22 g, 7 weeks old) were supplied by the First Clinical College Experimental Animal Center of Wuhan University. The animal experiments of this project were ethically approved by the Bioethics Committee of Renmin Hospital of Wuhan University (WDRM20220902C). All mice were given adequate water supply, sufficient food, and on the 12 h light/dark cycle in strict accordance with Laboratory Animals Guidelines. After receiving 3 days of adaptive feeding, those mice underwent UUO or renal I/R model construction.

2.3. Model Construction of UUO and Renal I/R. In the UUO model, all mice were randomly divided into 4 groups: Sham, UUO, UUO+ sterile saline (NS), UUO+ cardamonin (CAD), and $n = 5$ per group. In order to anesthetize the mice, 0.2% of pentobarbital sodium (50 mg/kg) was injected intraperitoneally. After fully exposing the left kidney through a left abdominal incision, we ligated the upper third of the left ureter at two points with sterile 4−0 silk and cut between the surgical sutures in the UUO group. The sham operation means that the left ureter was manipulated but not ligated after the abdominal incision. Cardamonin (100 mg/kg/days) or vehicle (1.0 mL/days, sterile saline) was given by gavage for 7 days after UUO surgery in UUO + CAD or UUO + NS. The dosage was determined based on our dose-exploration experiments (Figure 1A,B). The mice were sacrificed 14 days after the surgery for necessary measurements and experiments.

In renal I/R surgery, all mice were randomly assigned to 4 groups: Sham, I/R, I/R + NS, I/R + CAD, and $n = 6$ per group. Most of the mice underwent renal I/R surgery as we did previously.[21] After anesthetizing the mice and exposing the surgical field, we utilized one noninvasive vascular clip to clamp the left kidney pedicle after the right kidney was removed in all I/R groups. Mice were subjected to 30 min of ischemia and 24 h of reperfusion, and those times were chosen because our previous study demonstrated that the kidney damage in this model was significant.[21] In the Sham group, only the right nephrectomy was performed without following ischemia of the left kidney. CAD (100 mg/kg) or vehicle (1.0 mL/days, sterile saline) was given by oral administration for 3 days before I/R injury in I/R + CAD or I/R + NS.

2.4. Assessment of Renal Function. Fresh blood of those experimental mice was applied to detect the levels of serum creatinine (Cr) as well as blood urea nitrogen (BUN) by referring to their instructions of commercial kits (Nanjing Jiancheng Bioengineering Institute, Nanjing, C011-2-1 and C013-2-1).

2.5. Histological Staining. Kidney tissues were obtained to be fixed in 4% paraformaldehyde followed by embeddedness in paraffin. Serial sections (4 μm thick) were prepared for Masson trichrome, Sirius red, and hematoxylin and eosin (H&E) staining. Two professional pathologists observed the degree of tubular dilatation, brush border absence, tubular necrosis, and tubular pattern formation. Kidney injury scores were rated on a scale of 0−4 (0, normal; 1, <25%; 2, 25−50%; 3, 50−75%; and 4, ≥75%). Sirius red positive area and tubulointerstitial fibrosis index were assessed by uninformed experts and quantified via Image J software.

2.6. Immunohistochemistry (IHC). IHC staining of corresponding renal tissues was conducted as formerly reported.[9] Target proteins were detected and analyzed by incubation with antibodies including E-cadherin (1:2000, 20874-1-AP, Proteintech Group), KIM-1 (1:100, 14971S, Cell Signaling), and caspase-3 (1:200, WL02117, Wanleibio). Selecting 6 nonoverlapping fields of every specimen quantified the average optical density (OD) through Image J software.

2.7. Cell Culture and H/R Injury Model. HK-2 cell line (human renal proximal tubular epithelial cell line) was purchased from the China Center for Type Culture Collection (CTCC, China) and cultured in DME/F12 medium containing 5% fetal bovine serum (FBS, Gibco) and 1% penicillin−streptomycin−-amphotericin B (Solarbio, Beijing, P7630). They were incubated in a constant-temperature incubator (5% CO_2, 74% N_2, 21% O_2) at 37 °C. The recombinant TGF-β1 protein was initially identified as a growth factor that induces the growth of rodent fibroblasts and was always selected to induce cells to construct in vitro fibrosis models of various diseases.[22,23] In order to induce renal fibroblasts in vitro, 5 ng/mL of TGF-β1 was selected to be added into cell plates followed by the administration of CAD (100 μM, dissolved in DMSO) 4 h later. HK-2 cells were collected for further experiments after 24 h of fibrosis induction.

The H/R injury model was constructed as described in detail before.[24] In summary, cultured cells in the H/R group were required to be incubated in ordinary medium (serum-free and glucose-free) and then placed in one three-gas incubator (5% CO_2, 1% O_2, 94% N_2) at 37 °C for 12 h of hypoxia. After this step of hypoxia, the applied ordinary medium in the H/R group needs to be replaced by the complete medium mentioned above for 4 h of reoxygenation. The configured cardamonin was replenished into the cell culture medium 24 h prior to the establishment of the H/R model.

2.8. Quantitative Real-Time PCR (qRT-PCR) Analysis. Total RNA in treated cells or kidney tissues was extracted by the application of RNA extraction kit (Servicebio, Wuhan, G3013) in accordance with standard procedures. After cDNA synthesis was accomplished by cDNA Synthesis Kit (Servicebio, Wuhan, G3333-100), qRT-PCR was performed in the reaction mix containing Universal Blue SYBR Green (Servicebio, Wuhan, G3326-05) by qPCR Detection System (Bio-

Rad). Sangon Biotech (Shanghai, China) designed and synthesized the primer sequences applied in this study, which are displayed in Supporting Tables S1 and S2. Relative mRNA levels were quantified and normalized by using $2^{-\triangle\triangle CT}$ method. β-actin and GAPDH are the internal reference of the fibrosis model and I/R model, respectively.

2.9. Western Blot Analysis. The routinely completed process in protein detection was as presented previously.[21] Briefly, the protein content quantification was performed by the utilization of Enhanced Bicinchoninic Acid (BCA) Protein Assay Kit (P0010, Beyotime, Shanghai) according to product instructions once the protein was extracted. The total amount of 30 μg of unmeasured protein was separated through 10% sodium dodecyl sulfate-polyacrylamide gels (SDS-PAGE) followed by being transferred onto PVDF membranes. Protein Free Rapid Blocking Buffer (Epizyme, Shanghai, PS108P) was engaged in blocking PVDF membranes for 30 min at room temperature; then, membranes were immediately incubated in diluted specific primary antibodies including α-SMA (1:800, bs-0189R, Bioss Antibodies), collagen I (1:600, bs-10423R, Bioss Antibodies), β-actin (1:1500, GB11001, Servicebio), collagen III (1:1200, bs-0948R, Bioss Antibodies), fibronectin (1:1000, 15613-1-AP, Proteintech Group), Bcl-2 (1:3000, 26593-1-AP, Proteintech Group), P53 (1:5000, 10442-1-AP, Proteintech Group), GAPDH (1:1500, GB15004, Servicebio), BAX (1:6000, 50599-2-Ig, Proteintech Group), caspase-3 (1:600, WL02117, Wanleibio), TNF-α (1:600, 17590-1-AP, Proteintech Group), IL-6 (1:700, bs-0782R, Bioss Antibodies), IL-1β (1:1000, 16806-1-AP, Proteintech Group), catalase (1:3000, 21260-1-AP, Proteintech Group), SOD1 (1:7000, 10269-1-AP, Proteintech Group), SOD2 (1:8000, 24127-1-AP, Proteintech Group), phospho-IκBα (1:1500, #AF2002, Affinity), IκBα (1:1200, #AF5002, Affinity), KIM-1 (1:1000, AF1817, R&D Systems), NGAL (1:800, #DF6816, Affinity), NF-kb p65 (1:1500, #AF5006, Affinity), phospho-NF-kB p65 (1:500, #AF2006, Affinity), p38 (1:1500, 14064-1-AP, Proteintech Group), phospho-p38 (1:1200, 28796-1-AP, Proteintech Group), ERK (1:3000, #AF0155, Affinity), phospho-ERK (1:1000, #AF1015, Affinity), JNK (1:800, #AF6318, Affinity), and phospho-JNK (1:500, #AF3318, Affinity) antibodies overnight at 4 °C. Then, membranes were infiltrated with secondary goat anti-mouse or goat anti-rabbit antibody (1:4000, SA00001-1, SA00001-2, Proteintech Group) for 1 h of incubation at room temperature. GAPDH and β-actin are the commonly used loading controls in renal I/R injury and renal fibrosis in our previous studies, respectively.[9,22] Those blots were visualized with Chemiluminescent HRP Substrate (Epizyme, Shanghai, SQ201) and analyzed through the operation in Image Lab Software (NIH).

2.10. Cell Viability Assay. Cell viability of differently treated HK-2 cells in diverse groups was assessed by Cell Counting Kit-8 (Beyotime, Shanghai, C0038). In conclusion, the 5×10^3 cells/well were inoculated into 96-well plates for 24 h and then subjected to a variety of treatments. After the addition of 10 μL of CCK-8 reagent per well, HK-2 cells continued to receive incubation for 90 min in the dark. Cell viability was determined depending on the absorbance at 450 nm through the microplate reader.

2.11. Reactive Oxygen Species (ROS) Detection. Cellular ROS levels were measured by the usage of ROS Assay Kit obtained from Beyotime (S0033S, Shanghai). Dichlorodihydrofluorescein diacetate (DCFH-DA) was diluted in a serum-free medium at a ratio of 1:1000 to a final concentration of 10 μmol/L. The cell culture medium was removed, and an appropriate volume of diluted DCFH-DA was added. 2 mL of diluted DCFH-DA was usually added to per well of the six-well plates. HK-2 cells were incubated in an incubator at 37 °C for 30 min and washed 3 times with serum-free medium to fully remove the DCFH-DA that did not enter into cells. A fluorescence microscope was required to observe its fluorescence intensity, and Image J (NIH) software performed quantitative analysis.

2.12. Assessment of Antioxidant Enzyme Activities. Catalase and superoxide dismutase (SOD) activities were determined through relevant commercial kits provided by the Nanjing Jiancheng Institute of Biotechnology (A007-1 and A001-3, Nanjing) by acting in accordance with detailed instructions, while glutathione (GSH) concentration and MDA levels were detected by applicable assay kits (Beyotime, Shanghai, S0053 and S0131S) according to the operation instruction.

2.13. Hydrogen Peroxide (H_2O_2) Detection. Hydrogen Peroxide Assay Kit supplied by Beyotime (Shanghai, S0038) was applied to evaluate the H_2O_2 content in the kidney. Tissue samples were added with RIPA lysate at 10 μL/mg followed by centrifugation at 4 °C for 5 min at approx. 12,000 g/min, and the supernatant was removed for subsequent assays. Absorbance at 560 nm was measured after the addition of the detection reagent.

2.14. Measurement of Caspase-3 Activity. For the detection of caspase-3 enzyme activity in cells or tissue lysates, caspase-3 activity assay kit (Beyotime, Shanghai, C1116) was purchased and applied by referring to the manufacturer's instructions.

2.15. TUNEL (TdT-Mediated dUTP Nick-End Labeling) Staining. TUNEL Apoptosis Assay Kit was purchased from Beyotime (C1088, Shanghai, China). TUNEL assay of mice kidney was applied into implementation as formerly reported.[25] Briefly, deparaffinized and permeabilized sections of renal tissues were mixed with the TUNEL assay solution and incubated for 1 h without illumination. The average 10 random fields of each sample were observed to quantify the apoptotic degree.

2.16. Flow Cytometry. Phosphate-buffered saline (PBS) 1× buffer was utilized to wash the diversified treated HK-2 cells, and 1×10^4 cells were gathered and sequentially added with 195 μL of binding buffer, 5 μL of Annexin V-FITC, and 10 μL of propidium iodide (PI). After incubation in the dark for 20 min, apoptotic cells were figured out by a FACS flow cytometer (Bio-Rad).

2.17. Bioinformatics Analysis. *2.17.1. Drug Target Prediction.* The predicted targets of cardamonin were acquired from SwissTarget-Predition (http://www.swisstargetprediction.ch/) and HERB website (http://herb.ac.cn/). Gene names of all targets were matched and normalized through the UniProt database (https://www.uniprot.org/).

2.17.2. Acquisition of Disease Target. The renal I/R-related expression profiling by array GSE172042 and the UUO-related expression profiling by array GSE156181 were downloaded from the National Center for Biological Information-Gene Expression Omnibus (GEO, https://www.ncbi.nlm.nih.gov/geo/) database. Differentially expressed genes (DEGs) of GSE172042 and GSE156181 were analyzed using the Limma package of R software (GEO2R) according to a cutoff value "$P < 0.05$". Further, the intersection between CAD targets, GSE172042-related DEGs, and GSE156181-related DEGs was performed by Venny 2.1.0 Software (https://bioinfogp.cnb.csic.es/tools/venny/).

2.17.3. Functional Enrichment Analysis. Gene ontology and KEGG pathway analysis were carried out through Metascape analysis resource (https://metascape.org/) and visualized by the Bioinformatics website (https://www.bioinformatics.com.cn/). Heatmap was plotted by the Bioinformatics website as well.

2.17.4. Protein−Protein Interaction (PPI) Network. Intersected DEGs from CAD, GSE172042, and GSE156181 were entered into GENEMANIA (http://genemania.org/) to determine the PPI network.

2.18. Statistical Analysis. All results obtained from cellular and animal experiments were expressed as mean ± standard deviation (SD) and quantified using GraphPad Prism version 8.0 (CA). The Shapiro−Wilk test and Levene's test were selected to evaluate the data normality and variance homogeneity, respectively. The comparison between the two groups demanded to be identified by a two-tailed unpaired Student's *t* test. The Mann−Whitney test was performed to analyze 2 unpaired, non-normally distributed data points. The distinction among multiple groups was calculated employing a one-way ANOVA analysis of variance followed by Dunnett's post hoc test. *P* value <0.05 represented the statistical difference.

3. RESULTS

3.1. Cardamonin Application Remarkably Alleviated Acute Kidney Injury Induced by Renal I/R Surgery in Mice. First, in order to obtain an appropriate dosage for drug administration, we observed the consequence of CAD dose gradient on renal function by continuous gavage for 7 days and selected the dose at 100 mg/kg/days as believed by experimental
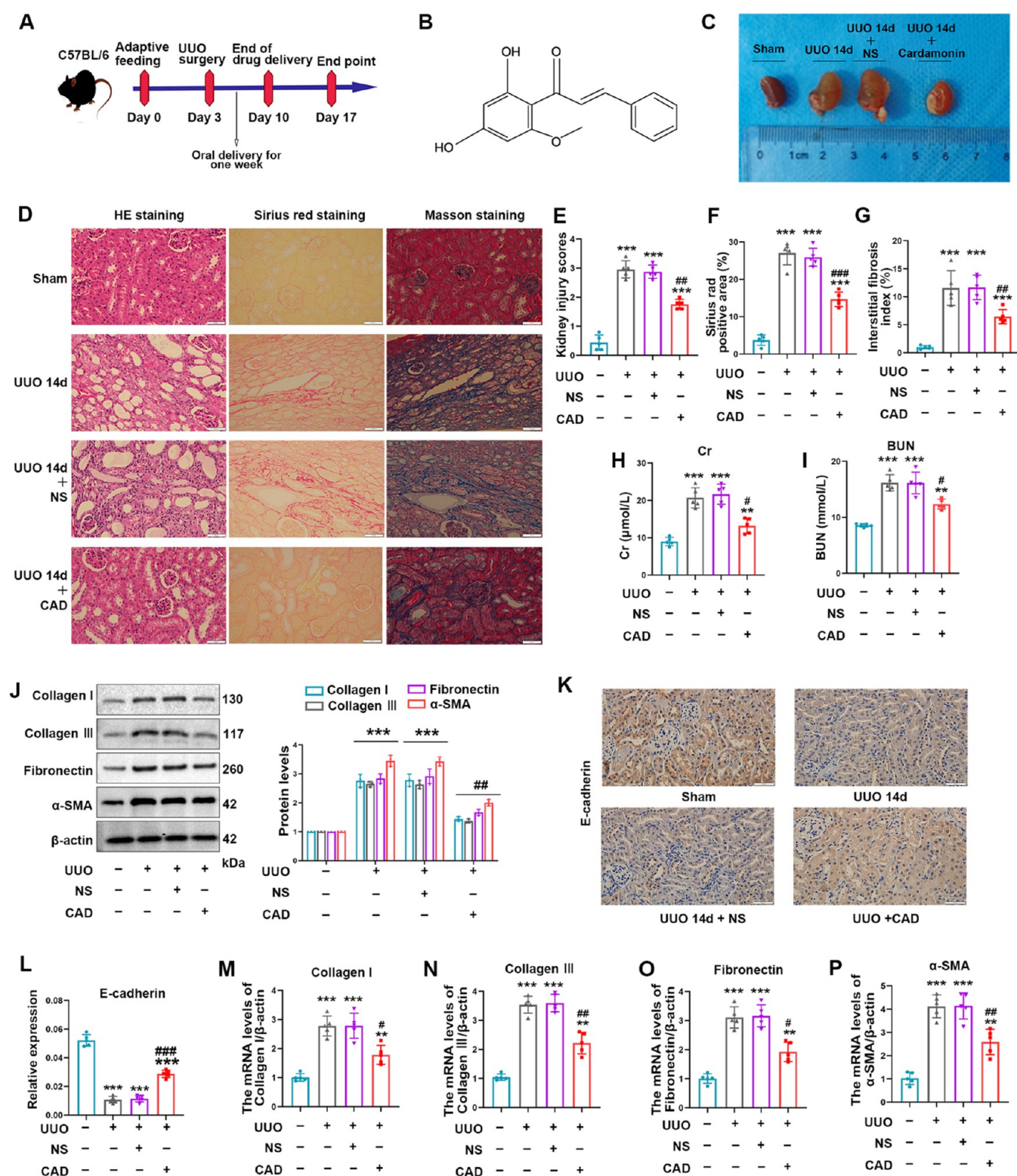
Figure 2. Cardamonin treatment ameliorated renal fibrogenesis induced by UUO exposure in mice. (A) Schematic diagram of cardamonin administration by gavage in animal experiments. (B) The structural formula of cardamonin. (C) Kidney size and morphology of mice in groups. (D−G) Representative images (400×, scale bar = 50 μm) and quantitative analysis of H&E, Sirius red, and Masson staining in kidneys of four animal groups. (H−I) Elevated levels of Cr and BUN declined in the UUO + CAD group compared with those of the UUO + NS group. (J) Western blot analysis was applied to detect the relative levels of fibrosis biomarkers including collagen I, collagen III, fibronectin, and α-SMA. (K, L) Representative images (400×, scale bar = 50 μ m) of immunohistochemical staining and quantitative analysis of E-cadherin in the corresponding groups. (M−P) Relative mRNA levels of collagen I, collagen III, fibronectin, and α-SMA in different groups. Measurement data from animal experiments were expressed as mean ± SD, n = 5 per group. *$P < 0.05$, **$P < 0.01$, and ***$P < 0.001$ vs Sham. #$P < 0.05$, ##$P < 0.01$, and ###$P < 0.001$ vs UUO.
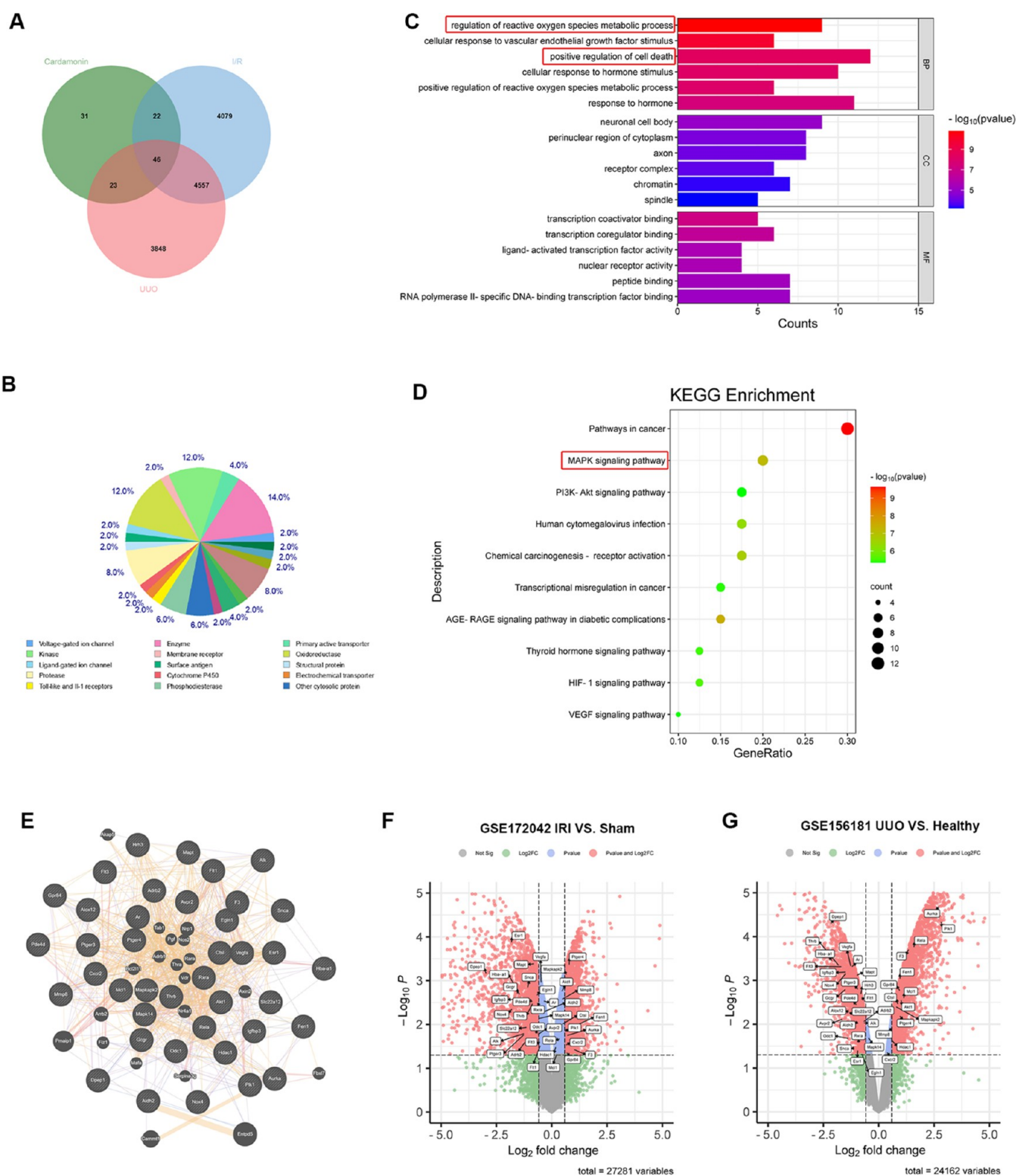
Figure 3. Bioinformatics analysis of target prediction and microarray data of renal I/R and UUO-related DEGs. (A) Venn diagram of cardamonin targets intersecting with renal I/R (GSE172042) and UUO (GSE156181)-associated DEGs. (B) Target classes of cardamonin's top 50 predicted targets via SwissTargetPrediction. (C) GO functional annotation of intersecting genes from drug and disease targets. (D) KEGG pathways of enriched DEGs. (E) Interaction network of DEGs via GeneMANIA. (F, G) Volcano Map displayed relevant DEGs in GSE172042 and GSE156181.

data (Figure 1A,B). Gavage administration of CAD at 100 mg/kg did not have an influential effect on the statistical difference in liver and cardiac functions in mice (Supporting Figure 1). Figure 1C conveniently displays the research process in the renal I/R model, and Figure 1D indicates the kidney appearance in

relevant groups. By performing H&E staining, we clearly discovered that CAD application considerably relieved tissue damage as stated by a decreased brush border detachment, nuclear consolidation, and tubular epithelium swelling compared with the I/R group (Figure 1E,F). The variation of kidney
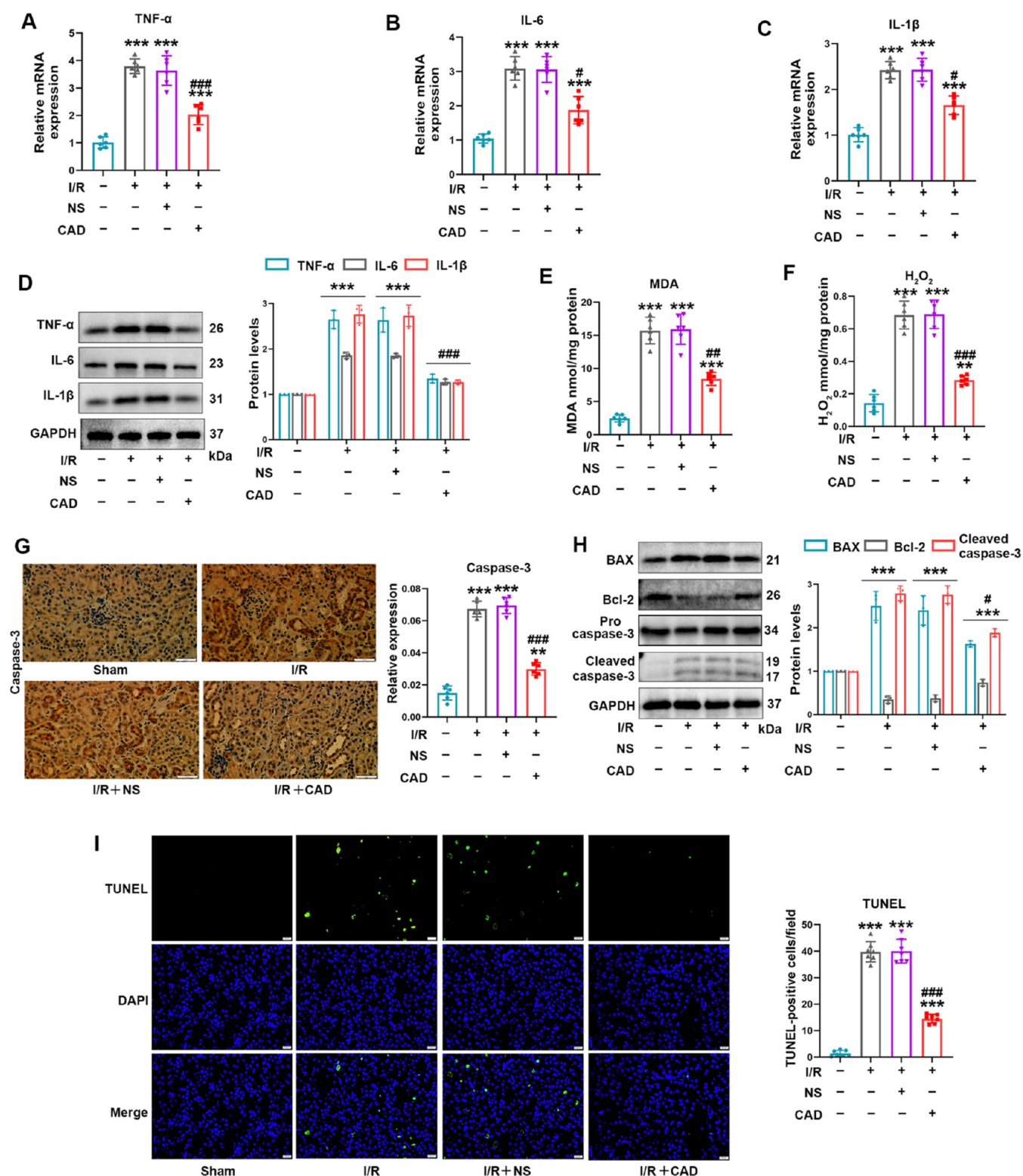
Figure 4. Cardamonin application distinctly prevented the activation of inflammation, oxidative stress, and apoptosis generated by renal I/R injury in vivo. (A−C) The mRNA expression of TNF-α, IL-6, and Il-1β was reduced after CAD application during I/R procedure. (D) The protein content of TNF-α, IL-6, and Il-1β was displayed. (E, F) The production of MDA and H_2O_2 was evaluated. (G) The caspase-3 expression in mice kidney was tested by IHC staining. (H) The apoptosis-associated markers consisting of BAX, Bcl-2, and cleaved caspase-3 were revealed by Western blot analysis. (I) The apoptosis degree was examined by TUNEL staining (400×, scale bar = 20 μm). Measurement data were expressed as mean ± SD, n = 6 per group. *$P < 0.05$, **$P < 0.01$, and ***$P < 0.001$ vs Sham. #$P < 0.05$, ##$P < 0.01$, and ###$P < 0.001$ vs I/R.

injury biomarkers remained consistent with the pathological lesion (Figure 1G,H). In addition, CAD treatment remarkably restrained the mRNA expression as well as protein levels of

kidney injury molecule-1 (KIM-1) and neutrophil gelatinase-associated lipocalin (NGAL) in Figure 1I−L. Immunohisto-chemistry staining manifested the upregulated generation of

KIM-1 in renal I/R-exposed mice, whereas CAD usage reversed the abnormal trend (Figure 1M).

3.2. Cardamonin Treatment Ameliorated Renal Fibrogenesis Induced by UUO Exposure in Mice. To gain an in-depth understanding of CAD's nephroprotective impact on the UUO injury, we successfully completed the surgical operation to establish the UUO model. The model process was rough as shown in Figure 2A. CAD's structural formula was displayed as well (Figure 2B). After completing the entire chronic model, we compared kidney appearance in diverse treatment groups, and what could be discovered was the apparent hydronephrosis and fibrotic thinning renal parenchyma in the kidneys 14 days after ureteral ligation. Encouragingly, the continuous oral administration of CAD for 7 days obtained a satisfactory outcome as displayed by the lessened hydronephrosis and more intact kidney contents in the UUO + CAD group (Figure 2C). The tubulointerstitial injury in mice generated by ureteral obstruction was verified by utilizing H&E staining, and interstitial ECM deposition could be incontrovertibly recognized in the positive area of Sirius red and Masson staining. Parallelly, taking CAD orally prevented the pronounced tissue damage as well as renal fibrosis in the UUO model (Figure 2D). Quantitative analysis of tissue injury scores and fibrosis staining positive areas are listed in Figure 2E−G. In agreement with tissue staining, specific kidney injury markers such as BUN and Cr also experienced a noticeable decline in the UUO + CAD group (Figure 2H,I). Additionally, positive indicators of fibrosis degree including collagen I, collagen III, fibronectin, and α-SMA went through the conspicuous upregulation in the UUO surgery.[8] Nevertheless, CAD delivery by gavage reversed the alteration trend of protein expression in those markers (Figure 2J). E-cadherin, the momentous epithelial marker, usually was lost in the proceeding of renal fibrosis, but its constrained level was rescued by CAD usage (Figure 2K,L). Moreover, the increased mRNA levels of the mentioned positive indicators were efficiently limited in the UUO + CAD group (Figure 2M,P).

3.3. Bioinformatics Analysis of Target Prediction and Microarray Data of Renal I/R and UUO-Related DEGs. In summary, animal experiments provided valid results that CAD treatment displayed beneficial protection effects against renal I/R surgery and UUO model in mice. To explore the underlying mechanisms and pathways responsible for the nephroprotective effects of CAD, we employed the "ingredient−target−pathway−disease" interactive network to conclude the regulated pathological processes and signaling pathways of CAD during renal I/R and UUO injuries.

A total of 122 unrepeated target genes of CAD were acquired from 100 predicted genes of SwissTargetPrediction and 33 potential targets of HERB. Next, RNA-sequencing data of mice samples underwent renal I/R and UUO models, which were acquired from the GEO database. The Limma package of R software (GEO2R) was applied to figure out the renal I/R (GSE172042) and UUO (GSE156181)-associated DEGs based on the following cutoff value "$P < 0.05$". A total of 9982 and 8474 relevant DEGs were identified from GSE172042 and GSE156181, respectively. Through Venny 2.1 software, 46 common genes were intersected between CAD targets, GSE172042-relevant DEGs, and GSE156181-associated DEGs (Figure 3A). Target classes of predicted top 50 potential targets from SwissTargetPrediction are shown in Figure 3B. Among those 46 intersected genes, a total of 6 genes (Ptk2, Ntrk2, Pdgfra, Prkca, Tnnc1, Car2) displayed opposite trend changes in

the data sets of renal I/R (GSE172042) and UUO (GSE156181). The remaining 40 genes with consistent trends were selected for GO and KEGG analyses through Metascape Analysis Resource. The GO term analysis (Figure 3C) revealed that those DEGs were mainly enriched in biological processes (BPs) such as the regulation of reactive oxygen species metabolic process, cellular response to vascular endothelial growth factor stimulus, and positive regulation of cell death. These DEGs were enriched in cellular components (CC) including neuronal cell body, perinuclear region of cytoplasm, and axon. Molecular functions (MFs) were principally enriched in the transcription coactivator binding, transcription coregulator binding, and ligand-activated transcription factor activity. The KEGG enrichment analysis (Figure 3D) proved that those 40 intersected genes were primarily enriched in pathways in cancer, MAPK, PI3K-Akt, human cytomegalovirus infection, chemical carcinogenesis-receptor activation pathways, etc. However, the PI3K-Akt pathway activation was testified to protect against the renal I/R injury and to promote the occurrence of renal fibrosis.[24,26] Interestingly, the MAPK signaling pathway played a consistent role in the progression of renal I/R and UUO injuries, despite significant differences in the mechanisms of the occurrence and development of acute and chronic kidney diseases. Inhibiting the phosphorylation of MAPK (p38, ERK, and JNK) obviously alleviated kidney damage induced by AKI or renal fibrosis through restraining inflammation and apoptosis.[26,27] Furthermore, the PPI network of 40 enriched common targets was analyzed via GENEMANIA (Figure 3E). Volcano Map displayed the expression of relevant intersected DEGs in GSE172042 and GSE156181 (Figure 3F,G).

3.4. Cardamonin Application Distinctly Prevented the Activation of Inflammation, Oxidative Stress, and Apoptosis Generated by Renal I/R Injury In Vivo. The above bioinformatics analysis implicated that CAD's predicted targets in renal I/R and UUO were primarily enriched in regulating oxidative stress, cell death, MAPK signaling pathway, etc. Since inflammation, oxidative stress, and apoptosis are the crucial and common pathological processes of AKI or CKD,[28] and the outstanding impact on the inhibition of those paradoxical procedures by cardamonin,[13] we figured out whether CAD exerted its beneficial role by mitigating them in renal I/R surgery. As expected, CAD application remarkably restrained the mRNA and protein expression of the key inflammation cytokines consisting of TNF-α, IL-6, and Il-1β in the I/R + CAD group through qRT-PCR and Western blot analysis (Figure 4A−D). The typical products of oxidative stress such as MAD and H_2O_2 were restrained obviously after CAD utilization during I/R surgery (Figure 4E,F). Furthermore, CAD usage considerably improved the apoptosis in mice kidneys subjected to I/R injury, as displayed by the inhibited expression of caspase-3 by IHC staining (Figure 4G), the reversed protein content of apoptosis-related markers (BAX, Bcl-2, cleaved caspase-3) through Western blot analysis (Figure 4H), and the downregulated positive area of TUNEL staining (Figure 4I) in the I/R + CAD group.

3.5. Cardamonin Application Clearly Relieved H/R Injury through Inhibiting Inflammation, Oxidative Stress, and Apoptosis In Vitro. To verify CAD's nephroprotective role in I/R exposure again, the H/R model in vitro was constructed. CCK-8 assay was employed to figure out an appropriate concentration of CAD in vitro. CAD at 100 μM was selected due to its no change in cell viability (Figure

Figure 5. Cardamonin application clearly relieved H/R injury by inhibiting inflammation, oxidative stress, and apoptosis in vitro. (A) Effects of different concentrations of CAD on cell viability were detected by CCK-8 assay. (B) Schematic diagram of CAD usage in HK-2 cells with the H/R model construction. (C) CAD treatment improved impaired cell viability in the H/R group. (D−F) Relative mRNA levels of TNF-α, IL-6, and Il-1β were detected by the utilization of qRT-PCR. (G) Western blot analysis for the inflammation biomarkers including TNF-α, IL-6, and Il-1β and the protein quantitative analysis. (H) Intracellular ROS levels were identified by the DCFH-DA probe (100×, scale bar = 100 μm). (I) MDA content in
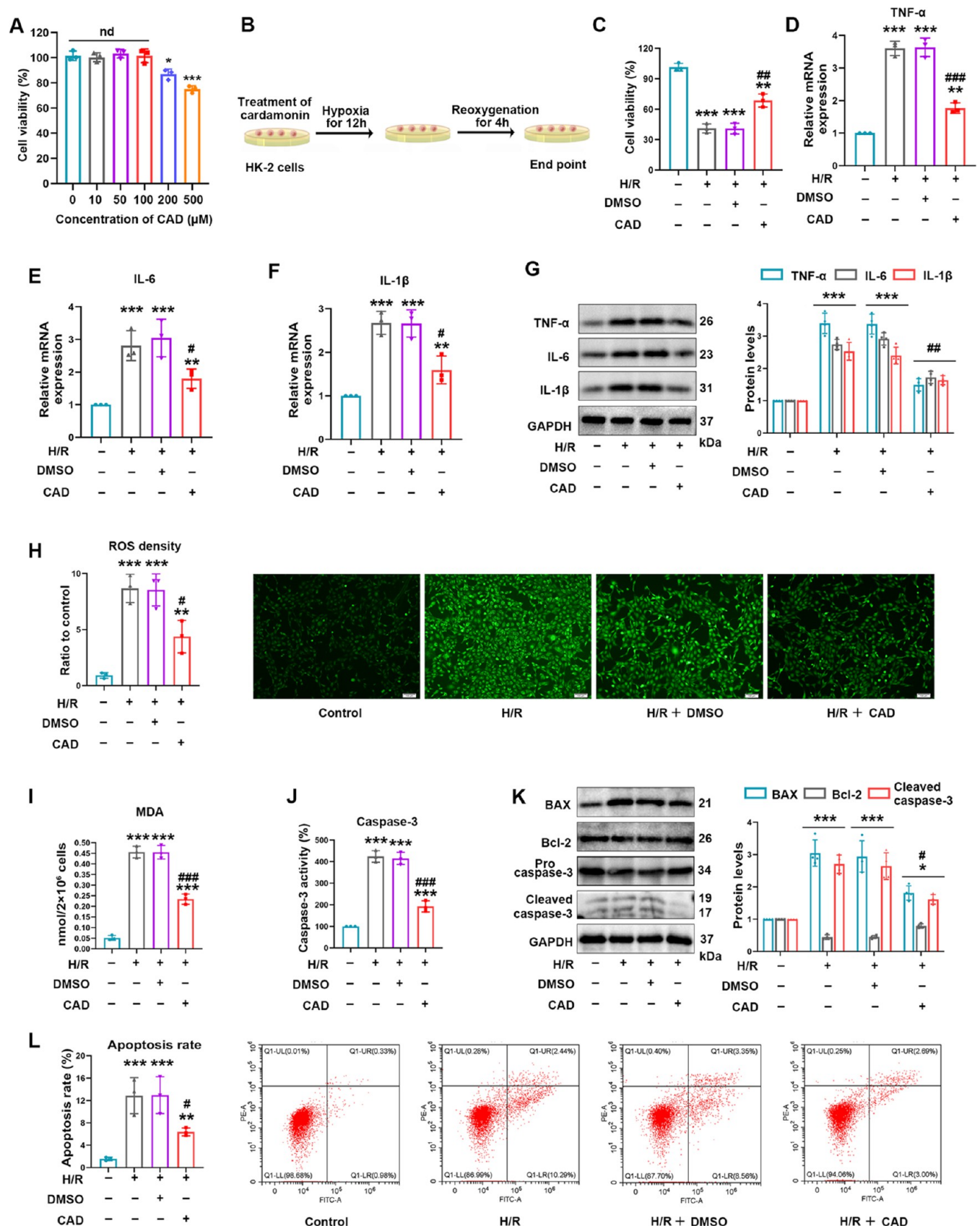
Figure 5. continued

HK-2 cells of corresponding groups. (J) Relative caspase-3 activity was measured in vitro. (K) The protein levels of cleaved caspase-3, Bcl-2, and BAX and displayed protein quantitative analysis. (L) Flow cytometry revealed the apoptosis rate in diverse handling groups. Measurement data were expressed as mean ± SD, n = 3 (3 times independent experiments). $*P < 0.05$, $**P < 0.01$, and $***P < 0.001$ vs control. $^{\#}P < 0.05$, $^{\#\#}P < 0.01$, and $^{\#\#\#}P < 0.001$ vs H/R.

5A). The H/R procedure of CAD treatment in HK-2 cells is exhibited in Figure 5B. CAD application prior to H/R exposure considerably altered H/R-impaired cell viability (Figure 5C). The inflammatory biomarkers, such as TNF-α, IL-6, and IL-1β, were demonstrated to be distinctively initiated in HK-2 cells undergoing H/R establishment. However, CAD utilization tremendously ameliorated the elevation in protein and mRNA expression of those markers as indicated by Western blot analysis and qRT-PCR (Figure 5D−G). Simultaneously, the intracellular DCFH-DA detection revealed the striking formation of ROS induced by establishing the H/R model, but CAD employment expressively prevented ROS generation (Figure 5H). In agreement with ROS levels, remarkable enlargement in the MDA content during H/R stimuli was noticeably suppressed after CAD administration (Figure 5I). Besides, apoptosis serving as the terminal event of tubular epithelial cell injury was unquestionably triggered during H/R injury. CAD utilization evidently restrained caspase-3 activity in HK-2 cells subjected to H/R injury (Figure 5J). Western blot analysis clearly manifested that Bcl-2 expression was rescued in the H/R + CAD group, and the amplified BAX and cleaved caspase-3 levels were greatly interrupted in the H/R + CAD group (Figure 5K). Flow cytometry illustrated the fact that the apoptosis rate displayed a doubtless upregulation under H/R stimuli; however, dealing with CAD overturned the trend during cellular experiments (Figure 5L).

3.6. Cardamonin Application Enhanced Antioxidative Capability and Inhibited the MAPK/NF-κB Signaling Pathway in Renal I/R and H/R Injuries. Our results verified that CAD administration effectively restrained oxidative products, inflammatory factors, and apoptotic events induced by renal I/R injury in vivo and in vitro. To uncover corresponding mechanisms behind CAD's performance in oxidation resistance and inflammation inhibition, we considered whether its beneficial role was related to crucial antioxidant enzymes and predicted pathways in Figure 3D. Importantly, previous reports repeatedly confirmed that CAD could enhance antioxidant capacity via upregulating antioxidant enzymes and inhibit inflammation through regulating MAPK or NF-κB signaling pathway to confer its positive role.[13,17−19,29,30] The MAPK/NF-κB pathway was frequently verified to regulate inflammation-induced apoptosis in various diseases.[31,32] Combining the existing reports and enrichment analysis in Figure 3, we detect the expression of the MAPK/NF-κB pathway, which was evidently activated during renal I/R injury as evidenced by the increased phosphorylation of p38, ERK, JNK, and NF-κB. However, CAD pretreatment clearly prevented the activation of the MAPK/NF-κB pathway in mice with renal I/R surgery (Figure 6A). Western blot analysis was taken to investigate how three major antioxidant genes altered in mice kidney with I/R damage. The results testified the decreased protein levels in SOD1, catalase, and SOD2 during I/R surgery, whereas CAD recovered the content in the I/R+CAD group compared with that in the I/R group (Figure 6B). In this research, the renal I/R-induced noticeable repression in antioxidant enzymes and endogenous antioxidant GSH was demonstrated. Interestingly,

CAD administration strikingly reversed the apparent depletion of SOD and catalase activity as well as GSG levels (Figure 6C−E). In HK-2 cells with the H/R model, CAD treatment elevated the protein levels of SOD1, catalase, and SOD2 and decreased the activation of the MAPK/NF-κB pathway as well (Figure 6F,G).

3.7. Cardamonin Treatment Mitigated Inflammation, Oxidative Stress, and Apoptosis Induced by UUO Exposure in Mice. Owing to the contributory role of inflammation, oxidative stress, and apoptosis in the pathogenesis of renal fibrosis,[33] we tested the corresponding biomarkers of them in vivo. The inflammation indicators including TNF-α, IL-6, and Il-1β were hampered during CAD exposure through the utilization of qRT-PCR and Western blot analysis (Figure 7A−D). CAD administration eliminated the excessive production of MDA and H_2O_2 in mice with the UUO model (Figure 7E,F). By performing the TUNEL assay, we could evidently witness that the tissue-positive apoptotic cells in the UUO group were reduced because of CAD employment (Figure 7G). In consistence with apoptosis alleviation, the caspase-3 expression was downregulated as well in the UUO + CAD group (Figure 7H). In addition, CAD treatment ameliorated the protein upregulation of apoptotic marker (P53, BAX, cleaved caspase-3) during renal fibrosis induced by UUO (Figure 7I).

3.8. Cardamonin Treatment Alleviated TGF-β1-Generated Fibrotic Injury by Inhibiting Inflammation, Oxidative Stress, and Apoptosis In Vitro. Subsequently, the TGF-β1 stimulation in HK-2 cells was carried out to validate the beneficial impact of CAD on renal fibrosis in vitro. Figure 8A illustrates the experimental procedure. Meanwhile, CAD application during the TGF-β1 exposure evidently alleviated fibrotic injury as indicated by the inhibition in protein and mRNA expression of mentioned biomarkers in the TGF-β1 + CAD group relative to that of the TGF-β1 group (Figure 8B−D). In addition, spindle-shaped, polygonal, and flattened star-shaped cell morphologies in the TGF-β1 group were improved a lot after CAD administration (Figure 8E). CAD employment remarkably blocked the TGF-β1-generated activation of proinflammatory cytokines consisting of TNF-α, IL-6, and Il-1β (Figure 8F−I). In line with ameliorating inflammation, CAD exertion possessed excellent performance in reducing ROS production and MDA overexpression (Figure 8J,K). Upregulated caspase-3 activity in HK-2 cells with TGF-β1 treatment was demonstrated to be repressed distinctly in the TGF-β1+CAD group (Figure 8L), along with a decline in key apoptotic markers (BAX, P53, cleaved caspase-3) (Figure 8M). CAD's restriction on TGF-β1-caused apoptosis was authenticated again by flow cytometry (Figure 8N).

3.9. Cardamonin Treatment Improved Antioxidative Capacity and Restrained the MAPK/NF-κB Signaling Pathway in UUO Model. In vitro, the activation of the MAPK/NF-κB pathway was effectively restrained as confirmed by the downregulated phosphorylation of p38, ERK, JNK, and NF-κB in the TGF-β1 + CAD group compared with that in the TGF-β1 group (Figure 9A). Since our previous study confirmed the critical role of three antioxidant enzymes in clearing
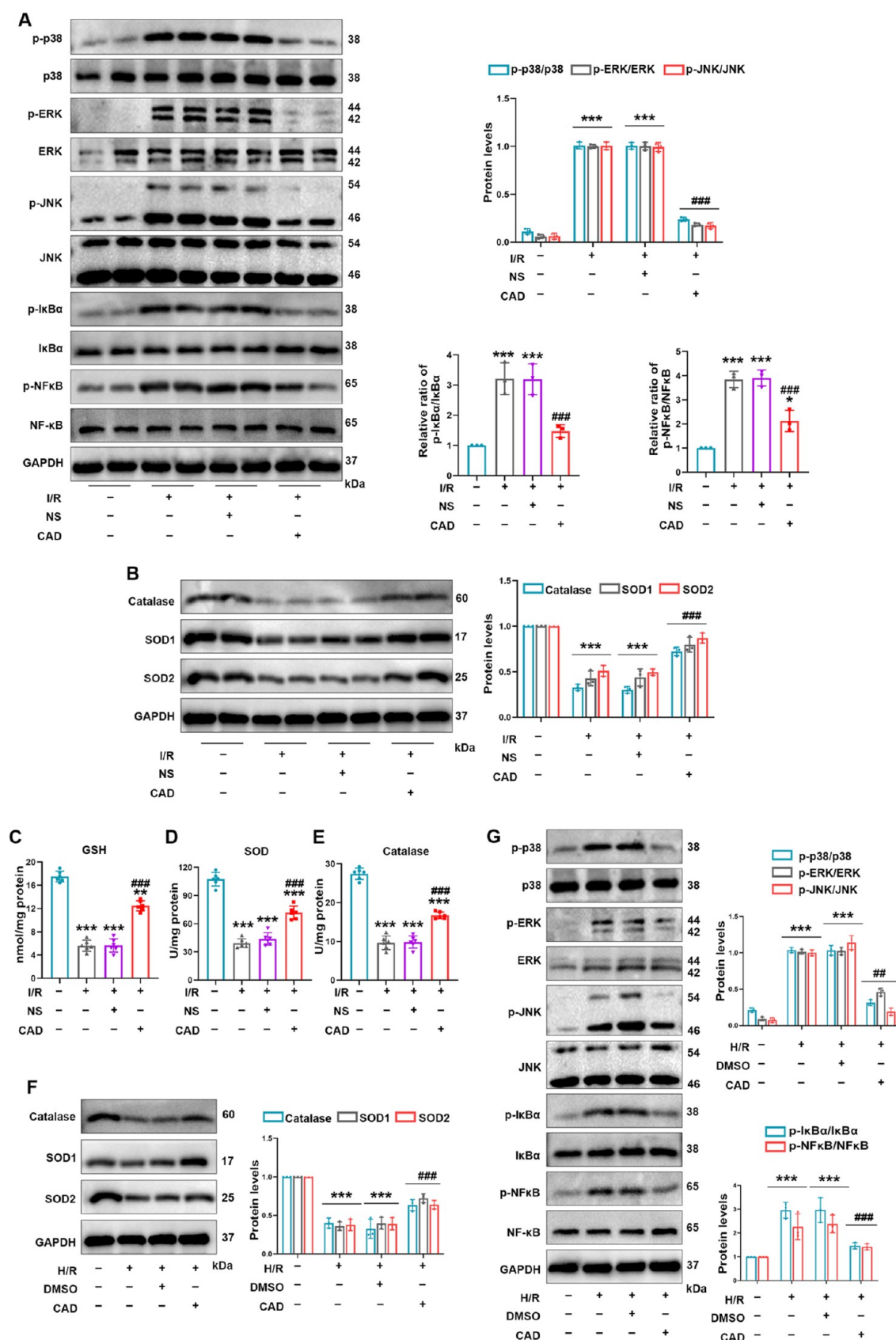
Figure 6. Cardamonin application enhanced the antioxidative capability and inhibited the MAPK/NF-κB signaling pathway in renal I/R and H/R injuries. (A) Western blot analysis detected the protein levels of p-p38, p38, p-ERK, ERK, p-JNK, JNK, p-IκBα, IκBα, p-NF-κB, and NF-κB in mice with I/R exposure. (B) CAD administration relieved the inhibition impact by I/R damage on protein levels of catalase, SOD1, and SOD2. (C) Renal GSH levels. (D, E) SOD and catalase activities in animal I/R experiments. (F) The protein levels of catalase, SOD1, and SOD2 in H/R model. (G) Western blot analysis of protein levels of the MAPK/NF-κB pathway in each group of HK-2 cells. Measurement data were expressed as mean ± SD, n =

Figure 6. continued

6 per group in mice; $n = 3$ (3 times independent experiments in HK-2 cells). $*P < 0.05$, $**P < 0.01$, and $***P < 0.001$ vs Sham or control. $^{#}P < 0.05$, $^{##}P < 0.01$, and $^{###}P < 0.001$ vs I/R or H/R.

produced harmful substances during oxidative stress,[34] we testified the protein levels of SOD1, catalase, and SOD2. Figure 9B indicates that CAD employment relieved TGF-β1's inhibition on those beneficial enzymes. Concurrently, the mice with CAD administration after ureteral ligation were favored with revitalized levels of GSH, SOD, and catalase activity (Figure 9C−E). Cardamonin recovered the protein levels of SOD1, catalase, and SOD2 in the UUO model as well (Figure 9F). The obstruction of the MAPK/NF-κB pathway during CAD utilization was determined in animal experiments (Figure 9G).

3.10. Schematic Illustration of Nephroprotective Effects of Cardamonin on Renal Ischemia Reperfusion Injury/UUO-Induced Renal Fibrosis. In summary, cardamonin restored the antioxidative capacity to block oxidative stress and suppressed the MAPK/NF-κB signaling pathway to alleviate inflammatory response, thus mitigating I/R-generated acute kidney injury/UUO-induced renal fibrosis in vivo and in vitro (Figure 10).

4. DISCUSSION

Acute kidney injury and chronic kidney disease are clinically intractable and complicated problems, and they are also interconnected in that AKI with unsatisfactory and delayed treatment could effortlessly progress to CKD, which dangerously ruins the patient's life quality.[1,2] The morbidity and mortality of patients who suffer from AKI or CKD with intricate clinical syndromes remain high, and what is more urgent and worrying is that the therapeutic outcome of numerous drugs is limited due to their toxic side effects and renal sensitivity in patients with impaired renal function.[2−4,35] Encouragingly, natural products identified from dietary agents evidently displayed outstanding advantages in chemical novelty, moderate toxicity, metabolic absorption, and biological effects in recent decades.[36,37] Cardamonin (Alpinetin chalcone), occurring naturally in the fruit of the Alpinia species, has been validated tautologically to exhibit noticeable anti-inflammatory and antioxidant activities in inflammatory diseases, acute injuries, and various tumors.[13−20] Nevertheless, the occurrence, progression, and pathogenesis of AKI and CKD differ from each other, whereas inflammation and oxidative stress are testified to be of vital importance in kidney diseases.[28] Meanwhile, a certain number of targeted drugs by inflammation inhibition and oxidative restriction were tested in clinical trials to figure out their potential in clinical application.[38,39] In view of the necessity of obtaining therapeutic targets for kidney diseases induced by AKI or CKD and the excellent biological efficacy of CAD, we innovatively investigated the consequence of CAD treatment on I/R-caused AKI and UUO-generated renal fibrosis in animal and cellular models. By performing histological staining and renal function assessment in this study, we clearly observed the depressed ECM deposition, improved kidney dysfunction, decreased tubular enlargement, and tubulointerstitial fibrosis after CAD oral application in the UUO model, and the repressed tissue damage, reduced expression in NGAL, KIM-1, Cr, or BUN in the CAD+I/R group. Interestingly, there existed a significant distinction in the kidney appearance

between the CAD group and control group during the research regarding I/R surgery or UUO exposure. In vitro, we again authenticated that CAD utilization improved the cell morphology and reduced the excessive expression of fibrotic markers such as collagen I, fibronectin, collagen III, and α-SMA during TGF-β1 stimulation. CAD employment also recovered the H/R-caused unsatisfactory cell viability. Therefore, employing CAD considerably protected kidney against I/R or UUO injury. To further validate the corresponding biological processes and signaling pathways of CAD's nephroprotective role, we collected CAD targets from SwissTargetPrediction and HERB, and we also downloaded RNA-sequencing data of renal I/R and UUO from the GEO database to construct the "ingredient−target−pathway−disease" interactive network. Functional enrichment analysis including Gene Ontology suggested that intersected genes were mainly enriched in BPs such as the regulation of reactive oxygen species metabolic process, cellular response to vascular endothelial growth factor stimulus, and positive regulation of cell death.

Oxidative stress (OS), specifically regulated by the oxidative/antioxidant system, was implicated in diverse kidney diseases. Destructive or persistent pathological circumstances stimulated the unrestrained formation of ROS, leading to harmful disturbance on antioxidative defense and distinguished repression of antioxidant enzymes (SOD, CAT, etc.).[28,40] Excessive and permanent OS inevitably triggered renal cell death by intensifying endoplasmic reticulum stress, pyroptosis, and apoptosis as testified by our published studies.[9,21,24,41] However, the regulatory mechanisms of oxidative stress in AKI or CKD are not absolutely identical despite the crucial participation of OS.[28,38−40] In recent years, relevant studies frequently demonstrated that suppressing OS would be capable of ameliorating renal fibrosis or AKI to a large extent.[8−10] Therefore, identifying and targeting the common pathways or molecules seem to be promising and necessary for treating kidney diseases.[2,7] Hopefully, some of the antioxidants and anti-inflammation regents have already been tested in clinical trials in patients with relevant kidney diseases and have exhibited encouraging end results. For example, Pablo E Pergola and his colleagues discovered that the oral administration of bardoxolone methyl, one modulator of antioxidant and anti-inflammation, upgraded the estimated glomerular filtration rate in patients along with type 2 diabetes and CKD at 24 weeks.[42] Taking curcumin orally for 3 months downregulated the levels of high-sensitivity C-reactive protein, inflammation-associated biomarkers, and NF-kB mRNA content in CKD patients with hemodialysis.[43] Intaking monomeric and oligomeric flavanols 14 days before ibuprofen/half-marathon obviously decreased the levels of urine markers such as IL-6 and MDA and diminished postrace hematuria incidence.[44] There are many more such clinical trials, which inspire researchers to continue to search for potential antioxidants and anti-inflammatory agents to prevent kidney diseases. In our investigation about renal I/R and UUO injuries, intaking CAD noticeably decreased the MDA and ROS contents and increased the levels of SOD and catalase activities accompanied by recognizable upregulated protein levels of SOD1, catalase, and SOD2. Our data validated that CAD could restore the activity of
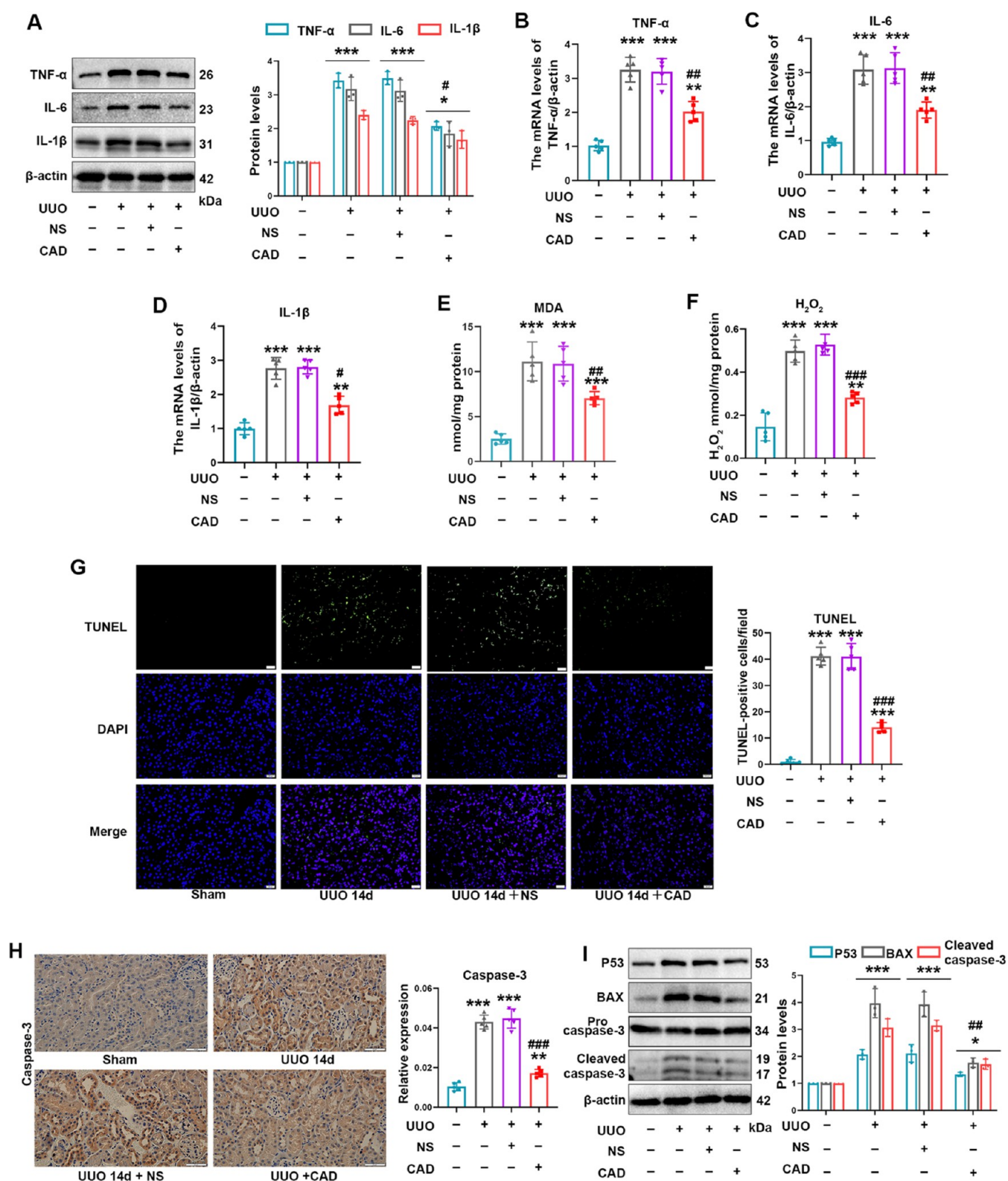
Figure 7. Cardamonin treatment mitigated inflammation, oxidative stress, and apoptosis induced by UUO exposure in mice. (A) Protein levels of inflammatory cytokines such as TNF-α, IL-6, and Il-1β in those indicated groups. (B–D) TNF-α, IL-6, and Il-1β mRNA levels in mice with assorted management. (E, F) The production of MDA and H_2O_2 was eliminated in the UUO + CAD group. (G) TUNEL staining on kidney sections (400×, scale bar = 20 μm). (H) Immunohistochemical staining of caspase-3 in mice kidney (400×, scale bar = 50 μm). (I) The protein levels of apoptotic markers including P53, BAX, and cleaved caspase-3 during UUO surgery. Measurement data from animal experiments were expressed as mean ± SD, n = 5 per group. *$P < 0.05$, **$P < 0.01$, and ***$P < 0.001$ vs Sham. #$P < 0.05$, ##$P < 0.01$, and ###$P < 0.001$ vs UUO.

crucial antioxidant enzymes to block oxidative stress in both I/R and UUO models. In addition, the influential outcome of SOD1,

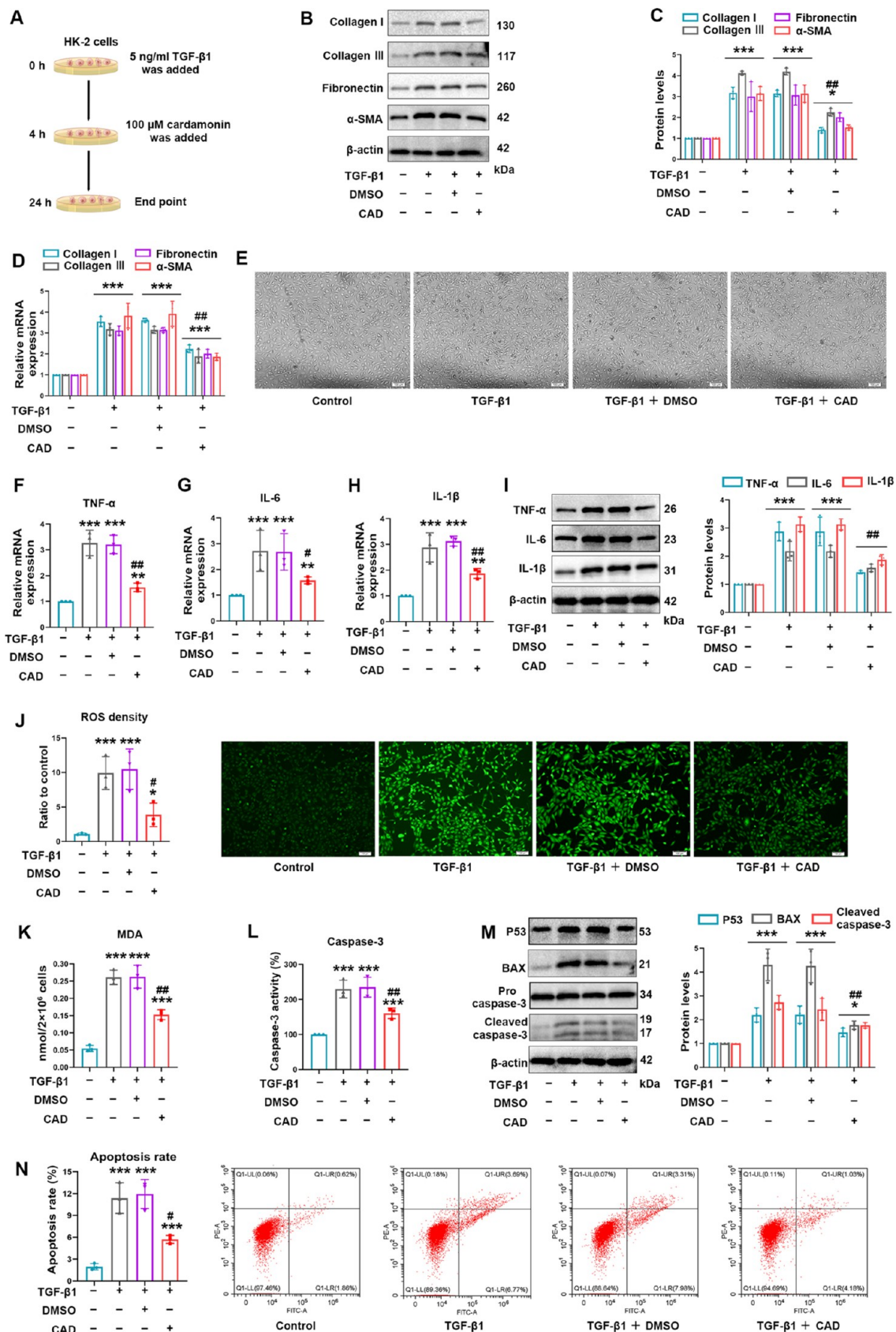catalase, and SOD2 on alleviating acute and chronic injuries was authenticated as well in our reports and others.[8,34]

Figure 8. Cardamonin treatment alleviated TGF-β1-generated fibrotic injury by inhibiting inflammation, oxidative stress, and apoptosis in vitro. (A) Schematic diagram of the CAD-treated cell model. (B, C) CAD application effectively inhibited the upregulated protein levels of collagen I, collagen III, fibronectin, and α-SMA during TGF-β1 exposure in HK-2 cells. (D) qRT-PCR explored the mRNA expression of collagen I, collagen III, fibronectin, and α-SMA. (E) Representative images (100×, scale bar = 100 μm) of cell morphology in relevant groups. (F−H) TNF-α, IL-6, and Il-1β mRNA levels in HK-2 cells. (I) Western blot analysis and quantification of TNF-α, IL-6, and Il-1β in vitro. (J) DCFH-DA probe detected intracellular

Figure 8. continued

ROS levels (100×, scale bar = 100 μ m), and the quantification was displayed. (K) MDA levels were quantified in HK-2 cells. (L) The caspase-3 activity in various groups. (M) Protein levels of apoptosis-related markers including BAX, P53, and cleaved caspase-3 in cellular models of fibrosis. (N) Flow cytometry clearly illustrated the role of CAD in attenuating apoptosis rate during TGF-β1 exposure. Measurement data from cellular experiments were expressed as mean ± SD, n = 3 (3 times independent experiments). *P < 0.05, **P < 0.01, and ***P < 0.001 vs control. #P < 0.05, ##P < 0.01, and ###P < 0.001 vs TGF-β1.

Inflammation is the basic pathological process of plentiful diseases and a defensive response made by the body for self-protection. However, an excessive inflammatory response will also cause serious harm to the body. In response to various kinds of stress, inflammatory factors such as TNF-α, IL-6, and Il-1β would be secreted to regulate local tissue and systemic reactions.[45] Inflammation is involved in multiple renal diseases induced by AKI or CKD and is implicated to be a meaningful and potential therapeutic target.[8,11,12,28,39] As mentioned above, a number of anti-inflammation agents have been practiced in clinical trials for kidney diseases with some success. According to prior reports, CAD has powerful anti-inflammatory properties in alleviating LPS-induced septic shock, osteoarthritis, colitis, and carrageenan-induced paw edema via inhibiting inflammatory factors, MAPK, and NF-κB signaling pathways.[15,16,29,46] In agreement with those findings, CAD occupied a crucial part in mitigating inflammatory cytokines consisting of TNF-α, IL-6, and Il-1β induced by UUO and I/R damage. Apoptosis caused by OS and inflammation during I/R or UUO injury in renal tissues and HK-2 cells was remarkably prevented as confirmed by IHC staining of caspase-3, caspase-3 activity measurement, TUNEL staining, flow cytometry, and apoptotic markers' protein levels.

Mitogen-activated protein kinase (MAPK), one serine/threonine kinase family that includes P38, ERK1/2, and JNK, was proven to regulate physiological activities including cell differentiation, inflammatory response, and cell death.[32] In response to acute or chronic kidney injury, the MAPK pathway was obviously activated as evidenced by the increased phosphorylation of P38, ERK1/2, and JNK, which exerts proinflammatory, proapoptotic, and profibrotic impacts during renal I/R injury and renal fibrosis.[47,48] Inhibiting the activation of the MAPK pathway was authenticated to significantly ameliorate AKI and renal fibrosis.[27,47,48] The enriched top 5 pathways of those 40 intersected genes in order are pathways in cancer, MAPK, PI3K-Akt, human cytomegalovirus infection, and chemical carcinogenesis-receptor activation pathways during KEGG enrichment analysis. The PI3K-Akt signaling pathway is not as consistent as the MAPK pathway in its role in renal I/R injury and renal fibrosis, whereas activating the PI3K-Akt pathway induced the process of TGF-β1-induced EMT and relieved renal I/R injury.[9,23] Previous studies revealed that CAD attenuated renal cyst enlargement, LPS-induced lung sepsis, and carrageenan-induced paw edema by inhibiting the MAPK signaling pathway.[17,29,30] The bioinformatic analyses and established studies seem to suggest that the MAPK signaling pathway participated in the regulation of renal I/R and UUO injuries during CAD administration. In our animal and cell models, CAD employment markedly mitigated the activation of MAPK NF-κB cascade to reduce renal I/R and UUO damage. These results are consistent with previous findings that restraining the MAPK/NF-κB pathway could ameliorate inflammation to relieve kidney injury.[49,50]

The pathophysiological mechanisms of renal I/R injury are complex and include calcium overload, microvascular endothe-

lial dysfunction, endoplasmic reticulum stress, autophagy, pyroptosis, and ferroptosis in addition to those mentioned above.[51] Among these, calcium overload is one of the major triggers during the ischemia/reperfusion stage. Rapid adenosine triphosphate (ATP) depletion induced by the ischemia stage inevitably leads to excessive aggregation of extracellular Ca^{2+} via activating Na^{+}−Ca^{2+} exchange channels and speeding cell membrane depolarization. Continuously increasing Ca^{2+} concentrations in the cytoplasm during the reperfusion stage severely disrupts the structure and function of crucial cell organelles including mitochondria, endoplasmic reticulum, etc., which in turn leads to cell death and induces AKI through various cascade reactions.[52,53] Abnormal biological processes during the I/R stage would also impair parenchymal cells including renal endothelium and deteriorate vascular function. Endothelial dysfunction induced by this endothelial damage in turn aggravates the reduction of organ blood flow during I/R through inflammatory response and changing vascular tone.[54] Previous reports suggested that ameliorating calcium overload and microvascular endothelial dysfunction will lessen I/R-generated renal damage.[53,54] The regulatory relationships of CAD on calcium overload and endothelial dysfunction are rarely reported, which also motivates us to figure out their relationship in future studies. The established studies validated CAD's biomedical properties in diversified disorders including ovarian cancer, cardiotoxicity, colon tumorigenesis, breast cancer, etc.[13,18] We originally figured out that CAD application could prevent the progression and end point of UUO or renal I/R surgery through anti-inflammatory and antioxidative authorities. Furthermore, the dosage employed in the treatment of pathological kidney diseases was safe and effective and did not deteriorate liver and cardiac functions in mice, demonstrating the low toxicity and excellent bioavailability of CAD, which alleviated our concerns about CAD's toxic and side effects in clinical application.

5. CONCLUSIONS

In summary, CAD administration remarkably improved the imbalanced antioxidant system and efficiently prevented the MAPK/NF-κB signaling pathway, thus ameliorating oxidative stress and inflammation to protect the kidney against I/R or UUO injury. These data indicated the application possibility of CAD in acute or chronic injury, as well as providing mechanistic insights for future clinical utilization. Although we successfully constructed models of renal I/R-induced AKI and UUO-generated renal fibrosis to verify CAD's protective impact on acute or chronic kidney injury in vivo and in vitro, we further validated the implicated regulatory mechanisms of CAD's nephroprotective effects via bioinformatics analysis and plentiful experiments. It is necessary to note that the direct targets and molecular docking of CAD action in kidney diseases need to be further completed in future studies.
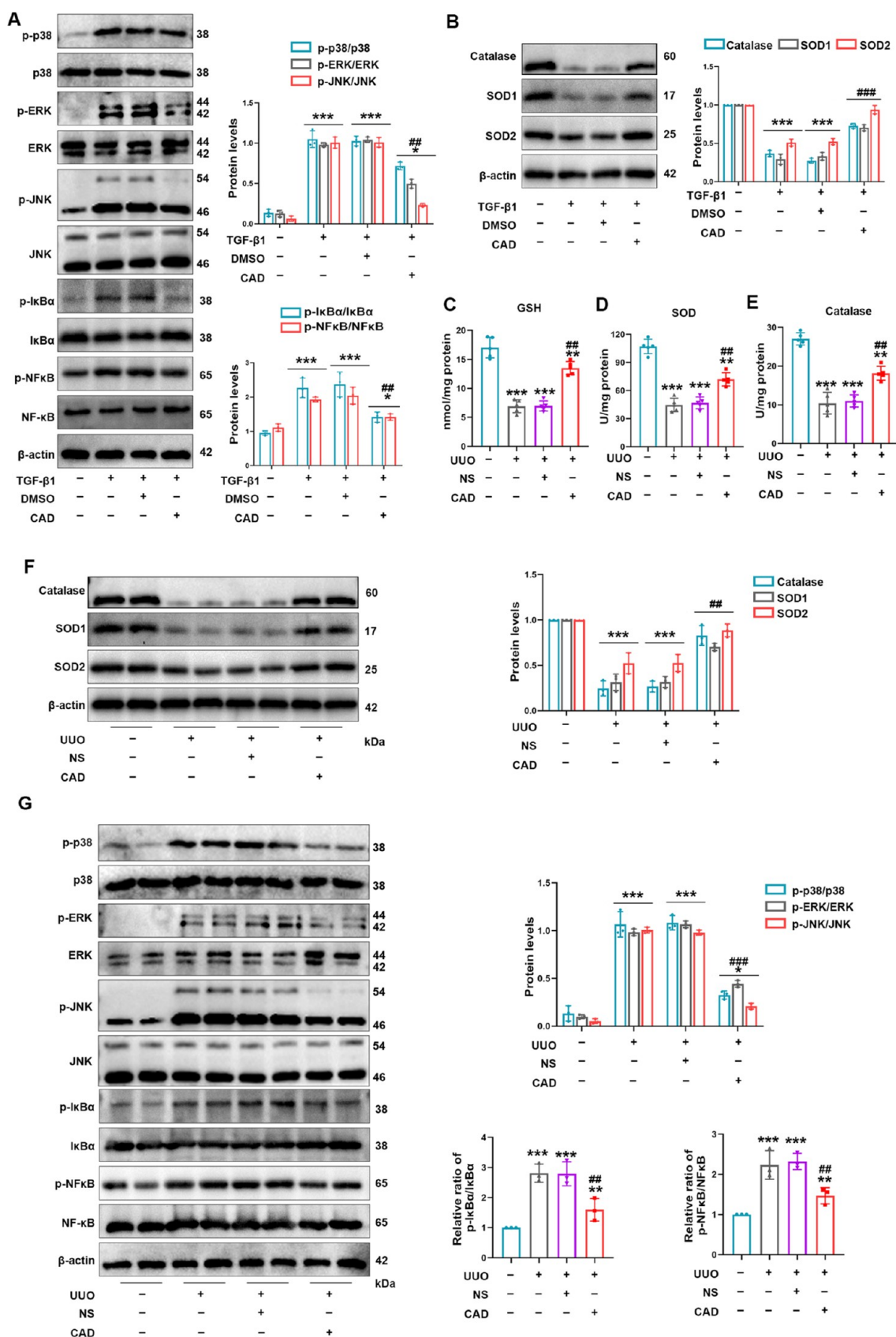
Figure 9. Cardamonin treatment improved the antioxidative capacity and restrained the MAPK/NF-κB signaling pathway in the UUO model. (A) CAD usage prevented the activation of p-p38/p38, p-ERK/ERK, p-JNK/JNK, p-IκBα/ IκBα, and p-NF-κB/NF-κB in TGF-β1-treated HK-2 cells. (B) CAD application restored the downregulated protein levels of catalase, SOD1, and SOD2 in HK-2 cells exposed to TGF-β1 stimulation. (C) GSH levels in kidney tissues. (D) SOD activities and (E) catalase activities in mice kidney were analyzed in related groups. (F) Protein levels of catalase, SOD1, and SOD2 in mice kidney were detected and quantified. (G) Western blot analysis of p-p38, p38, p-ERK, ERK, p-JNK, JNK, p-IκBα, IκBα, p-

Figure 9. continued

NF-κB, and NF-κB in each group of an animal model. Measurement data were expressed as mean $\pm$ SD, $n = 5$ per group in mice; $n = 3$ (three times independent experiments in HK-2 cells). $*P < 0.05$, $**P < 0.01$, and $***P < 0.001$ vs Sham or control. $^{\#}P < 0.05$, $^{\#\#}P < 0.01$, and $^{\#\#\#}P < 0.001$ vs UUO or TGF-β1.
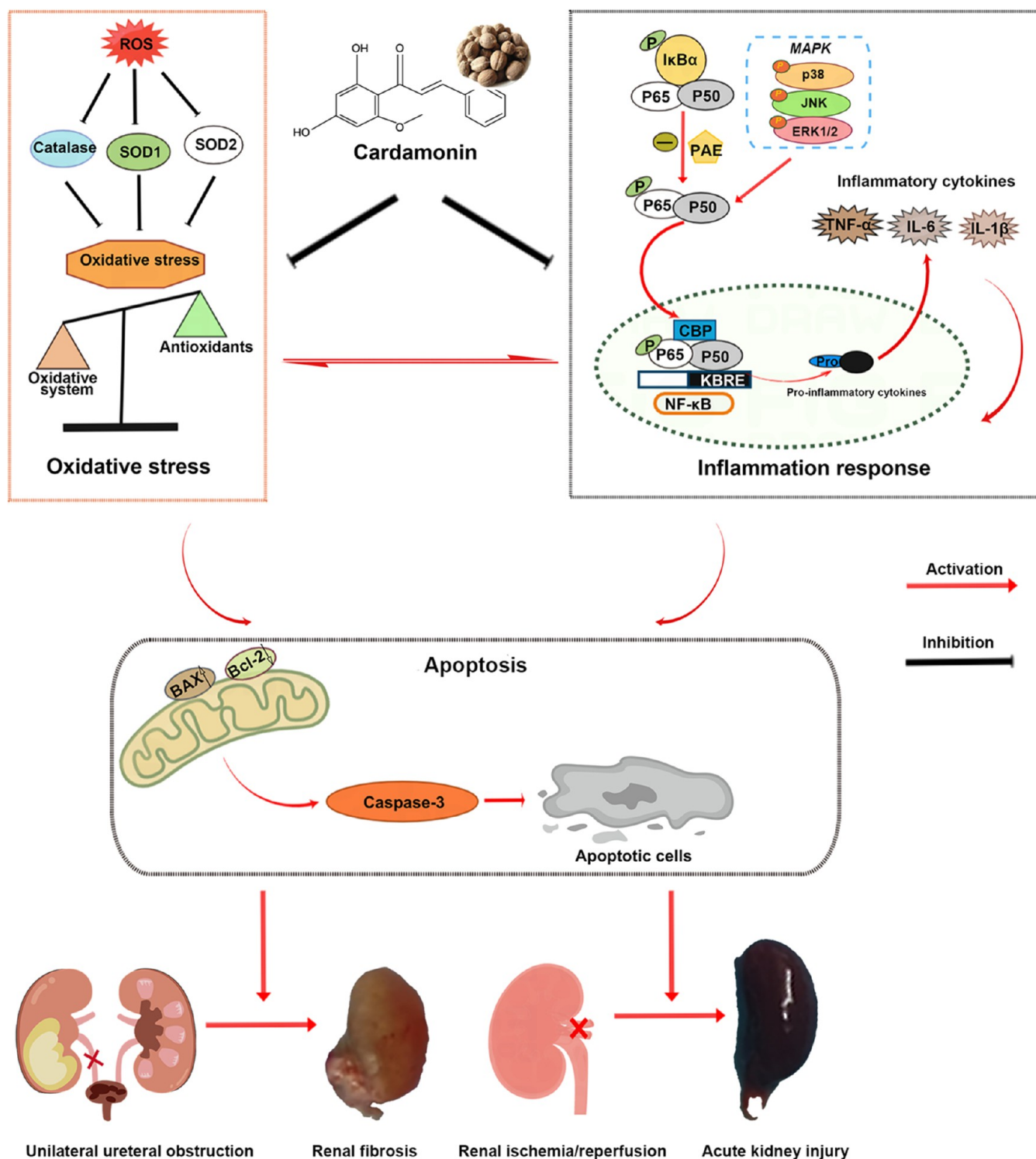

Figure 10. Schematic illustration of nephroprotective effects of cardamonin on renal ischemia reperfusion injury/UUO-induced renal fibrosis.

ASSOCIATED CONTENT

ⓢ Supporting Information

The Supporting Information is available free of charge at https://pubs.acs.org/doi/10.1021/acs.jafc.3c01880.

> Designed and synthesized primer sequences of human or mouse genes and the influence of 100 mg/kg/days of cardamonin by continuous gavage for 7 days on liver and heart function in mice (PDF)

AUTHOR INFORMATION

Corresponding Authors

Xiu-Heng Liu — *Department of Urology, Renmin Hospital of Wuhan University, Wuhan 430060, China; Wuhan University Institute of Urological Disease, Wuhan 430060, China;* Email: drwanglei@whu.edu.cn

Lei Wang — *Department of Urology, Renmin Hospital of Wuhan University, Wuhan 430060, China; Wuhan University Institute of Urological Disease, Wuhan 430060, China;* Email: drliuxh@hotmail.com

Authors

Banghua Zhang — *Department of Urology, Renmin Hospital of Wuhan University, Wuhan 430060, China; Wuhan University Institute of Urological Disease, Wuhan 430060, China; Hubei Key Laboratory of Digestive System Disease, Wuhan 430060, China;* ⓞ orcid.org/0000-0003-4367-901X

Zhi-Yuan Chen — *Department of Urology, Renmin Hospital of Wuhan University, Wuhan 430060, China; Wuhan University Institute of Urological Disease, Wuhan 430060, China*

Zhengyu Jiang — *Department of Urology, Renmin Hospital of Wuhan University, Wuhan 430060, China; Wuhan University Institute of Urological Disease, Wuhan 430060, China*

Shiyu Huang — *Department of Urology, Renmin Hospital of Wuhan University, Wuhan 430060, China; Wuhan University Institute of Urological Disease, Wuhan 430060, China; Hubei Key Laboratory of Digestive System Disease, Wuhan 430060, China*

Complete contact information is available at:
https://pubs.acs.org/10.1021/acs.jafc.3c01880

Author Contributions

∥B.Z. and Z.-Y.C. contributed equally to this work. X.-H.L., L.W., and Z.-Y.C. participated in the conceptualization, methodology, and funding acquisition of this study. B.Z. was responsible for the experimental implementation, draft writing, and figure visualization. Z.J. and S.H. contributed to data curation, formal analysis, and figure visualization.

Notes

The authors declare no competing financial interest.

ACKNOWLEDGMENTS

ABBREVIATIONS USED

UUO, unilateral ureteral obstruction; CAD, cardamonin; ESRD, end-stage renal disease; I/R, ischemia/reperfusion; MAPK, mitogen-activated protein kinase; ECM, extracellular matrix; H&E, hematoxylin−eosin; AKI, acute kidney injury; NGAL, neutrophil gelatinase-associated lipocalin; CKDs, chronic kidney diseases; DMSO, dimethyl sulfoxide; NS, sterile saline; KIM-1, kidney injury molecule 1; Cr, creatinine; PEG300, poly(ethylene glycol) 300; BUN, blood urea nitrogen; BAX, BCL-2-associated X protein; HK-2, human renal tubular epithelial cell line; Bcl-2, B-cell leukemia/lymphoma 2; CCK-8, cell counting kit 8; SD, standard deviation; MDA, malondialdehyde; HPLC, high-performance liquid chromatography; SOD2, superoxide dismutase 2; H/R, hypoxia/reoxygenation; LPS, lipopolysaccharide; SOD1, superoxide dismutase 1; ATP, adenosine triphosphate; IL-6, interleukin 6; IL-1β, interleukin 1,β

REFERENCES

(1) James, M. T.; Bhatt, M.; Pannu, N.; Tonelli, M. Long-term outcomes of acute kidney injury and strategies for improved care. *Nat. Rev. Nephrol.* **2020**, *16*, 193−205.

(2) Ronco, C.; Bellomo, R.; Kellum, J. A. Acute kidney injury. *Lancet* **2019**, *394*, 1949−1964.

(3) Peerapornratana, S.; Manrique-Caballero, C. L.; Gómez, H.; Kellum, J. A. Acute kidney injury from sepsis: current concepts, epidemiology, pathophysiology, prevention and treatment. *Kidney Int.* **2019**, *96*, 1083−1099.

(4) Hallan, S. I.; Vikse, B. E. Relationship between chronic kidney disease prevalence and end-stage renal disease risk. *Curr. Opin. Nephrol. Hypertens.* **2008**, *17*, 286−291.

(5) Luo, F.; Xu, R.; Song, G.; Xue, D.; He, X.; Xia, Y. Alleviation of TGF-beta 1 induced tubular epithelial-mesenchymal transition via the delta-opioid receptor. *FEBS J.* **2021**, *288*, 1243−1258.

(6) Su, H.; Wan, C.; Song, A.; Qiu, Y.; Xiong, W.; Zhang, C. Oxidative Stress and Renal Fibrosis: Mechanisms and Therapies. In *Advances in Experimental Medicine and Biology*; Liu, B. C.; Lan, H. Y.; Lv, L. L., Eds.; Springer, 2019; Vol., pp 585−604.

(7) Tampe, D.; Zeisberg, M. Potential approaches to reverse or repair renal fibrosis. *Nat. Rev. Nephrol.* **2014**, *10*, 226−237.

(8) Park, J. H.; Leem, J.; Lee, S. J. Protective Effects of Carnosol on Renal Interstitial Fibrosis in a Murine Model of Unilateral Ureteral Obstruction. *Antioxidants* **2022**, *11*, No. 2341.

(9) Liu, H.; Wang, L.; Weng, X. D.; Chen, H.; Du, Y.; Diao, C. H.; Chen, Z. Y.; Liu, X. H. Inhibition of Brd4 alleviates renal ischemia/reperfusion injury-induced apoptosis and endoplasmic reticulum stress by blocking FoxO4-mediated oxidative stress. *Redox Biol.* **2019**, *24*, No. 101195.

(10) Su, H.; Wan, C.; Song, A.; Qiu, Y.; Xiong, W.; Zhang, C. Oxidative Stress and Renal Fibrosis: Mechanisms and Therapies. *Adv. Exp. Med. Biol.* **2019**, *1165*, 585−604.

(11) Kimura, T.; Isaka, Y.; Yoshimori, T. Autophagy and kidney inflammation. *Autophagy* **2017**, *13*, 997−1003.

(12) Tang, P.-K.; Nikolic-Paterson, D. J.; Lan, H. Y. Macrophages: versatile players in renal inflammation and fibrosis. *Nat. Rev. Nephrol.* **2019**, *15*, 144−158.

(13) Nawaz, J.; Rasul, A.; Shah, M. A.; Hussain, G.; Riaz, A.; Sarfraz, I.; Zafar, S.; Adnan, M.; Khan, A. H.; Selamoglu, Z. Cardamonin: A new player to fight cancer via multiple cancer signaling pathways. *Life Sci.* **2020**, *250*, No. 117591.

(14) Bailly, C.; Vergoten, G. Mechanistic insights into dimethyl cardamonin-mediated pharmacological effects: A double control of the AMPK-HMGB1 signaling axis. *Life Sci.* **2020**, *263*, No. 118601.

(15) Wang, Z. L.; Xu, G.; Gao, Y.; Zhan, X. Y.; Qin, N.; Fu, S. B.; Li, R. S.; Niu, M.; Wang, J. B.; Liu, Y. P.; Xiao, X. H.; Bai, Z. F. Cardamonin from a medicinal herb protects against LPS-induced septic shock by suppressing NLRP3 inflammasome. *Acta Pharm. Sin. B* **2019**, *9*, 734−744.

(16) Peng, Y. J.; Lu, J. W.; Lee, C. H.; Lee, H. S.; Chu, Y. H.; Ho, Y. J.; Liu, F. C.; Huang, C. J.; Wu, C. C.; Wang, C. C. Cardamonin Attenuates Inflammation and Oxidative Stress in Interleukin-1beta-Stimulated

Osteoarthritis Chondrocyte through the Nrf2 Pathway. *Antioxidants* **2021**, *10*, No. 862.

(17) Yang, L.; Luo, W.; Zhang, Q.; Hong, S.; Wang, Y.; Samorodov, A. V.; Chattipakorn, N.; Pavlov, V. N.; Liang, G. Cardamonin inhibits LPS-induced inflammatory responses and prevents acute lung injury by targeting myeloid differentiation factor 2. *Phytomedicine* **2021**, *93*, No. 153785.

(18) Qi, W.; Boliang, W.; Xiaoxi, T.; Guoqiang, F.; Jianbo, X.; Gang, W. Cardamonin protects against doxorubicin-induced cardiotoxicity in mice by restraining oxidative stress and inflammation associated with Nrf2 signaling. *Biomed. Pharmacother.* **2020**, *122*, No. 109547.

(19) Peng, S.; Hou, Y.; Yao, J.; Fang, J. Activation of Nrf2-driven antioxidant enzymes by cardamonin confers neuroprotection of PC12 cells against oxidative damage. *Food Funct.* **2017**, *8*, 997−1007.

(20) Atef, Y.; El-Fayoumi, H. M.; Abdel-Mottaleb, Y.; Mahmoud, M. F. Effect of cardamonin on hepatic ischemia reperfusion induced in rats: Role of nitric oxide. *Eur. J. Pharmacol.* **2017**, *815*, 446−453.

(21) Zhang, B. H.; Wan, S. S.; Liu, H.; Qiu, Q. M.; Chen, H.; Chen, Z. Y.; Wang, L.; Liu, X. H. Naringenin Alleviates Renal Ischemia Reperfusion Injury by Suppressing ER Stress-Induced Pyroptosis and Apoptosis through Activating Nrf2/HO-1 Signaling Pathway. *Oxid. Med. Cell. Longevity* **2022**, *2022*, 1−24.

(22) Zhang, J.; Chen, H.; Weng, X.; Liu, H.; Chen, Z.; Huang, Q.; Wang, L.; Liu, X. RCAN1.4 attenuates renal fibrosis through inhibiting calcineurin-mediated nuclear translocation of NFAT2. *Cell Death Discov.* **2021**, *7*, No. 317.

(23) Hou, D.; Wu, Q.; Wang, S.; Pang, S.; Liang, H.; Lyu, H.; Zhou, L.; Wang, Q.; Hao, L. Knockdown of miR-214 Alleviates Renal Interstitial Fibrosis by Targeting the Regulation of the PTEN/PI3K/AKT Signalling Pathway. *Oxid. Med. Cell. Longevity* **2022**, *2022*, 1−17.

(24) Zhang, B.-H.; Liu, H.; Yuan, Y.; Weng, X. D.; Du, Y.; Chen, H.; Chen, Z. Y.; Wang, L.; Liu, X. H. Knockdown of TRIM8 Protects HK-2 Cells Against Hypoxia/Reoxygenation-Induced Injury by Inhibiting Oxidative Stress-Mediated Apoptosis and Pyroptosis via PI3K/Akt Signal Pathway. *Drug Des., Dev. Ther.* **2021**, *15*, 4973−4983.

(25) Tang, C.; Han, H.; Yan, M.; Zhu, S.; Liu, J.; Liu, Z.; He, L.; Tan, J.; Liu, Y.; Liu, H.; Sun, L.; Duan, S.; Peng, Y.; Liu, F.; Yin, X. M.; Zhang, Z.; Dong, Z. PINK1-PRKN/PARK2 pathway of mitophagy is activated to protect against renal ischemia-reperfusion injury. *Autophagy* **2018**, *14*, 880−897.

(26) Zhang, Y.; Jin, D.; Kang, X.; Zhou, R.; Sun, Y.; Lian, F.; Tong, X. Signaling Pathways Involved in Diabetic Renal Fibrosis. *Front. Cell Dev. Biol.* **2021**, *9*, No. 696542.

(27) Xu, X. J.; Zhang, M. L.; Hou, Y. M.; Zhang, K.; Yao, D. H.; Li, G. Y.; Kou, W. B.; Wang, H. Y.; Wang, J. H. The Amomum tsao-ko Essential Oils Inhibited Inflammation and Apoptosis through p38/JNK MAPK Signaling Pathway and Alleviated Gentamicin-Induced Acute Kidney Injury. *Molecules* **2022**, *27*, No. 7121.

(28) He, L.; Wei, Q.; Liu, J.; Yi, M.; Liu, Y.; Liu, H.; Sun, L.; Peng, Y.; Liu, F.; Venkatachalam, M. A.; Dong, Z. AKI on CKD: heightened injury, suppressed repair, and the underlying mechanisms. *Kidney Int.* **2017**, *92*, 1071−1083.

(29) Li, Y. Y.; Huang, S. S.; Lee, M. M.; Deng, J. S.; Huang, G. J. Anti-inflammatory activities of cardamonin from Alpinia katsumadai through heme oxygenase-1 induction and inhibition of NF-kappaB and MAPK signaling pathway in the carrageenan-induced paw edema. *Int. Immunopharmacol.* **2015**, *25*, 332−339.

(30) He, J.; Zhou, H.; Meng, J.; Zhang, S.; Li, X.; Wang, S.; Shao, G.; Jin, W.; Geng, X.; Zhu, S.; Yang, B. Cardamonin retards progression of autosomal dominant polycystic kidney disease via inhibiting renal cyst growth and interstitial fibrosis. *Pharmacol. Res.* **2020**, *155*, No. 104751.

(31) Wu, Y.; Duan, Z.; Qu, L.; Zhang, Y.; Zhu, C.; Fan, D. Gastroprotective effects of ginsenoside Rh4 against ethanol-induced gastric mucosal injury by inhibiting the MAPK/NF-kappaB signaling pathway. *Food Funct.* **2023**, *14*, 5167−5181.

(32) Zhao, J.; Zhang, R.; Wang, W.; Jiang, S.; Liang, H.; Guo, C.; Qi, J.; Zeng, H.; Song, H. Low-dose ketamine inhibits neuronal apoptosis and neuroinflammation in PC12 cells via alpha7nAChR mediated TLR4/

MAPK/NF-kappaB signaling pathway. *Int. Immunopharmacol.* **2023**, *117*, No. 109880.

(33) Nastase, M. V.; Zeng-Brouwers, J.; Wygrecka, M.; Schaefer, L. Targeting renal fibrosis: Mechanisms and drug delivery systems. *Adv. Drug Delivery Rev.* **2018**, *129*, 295−307.

(34) Liu, H.; Wang, W.; Weng, X.; Chen, H.; Chen, Z.; Du, Y.; Liu, X.; Wang, L. The H3K9 histone methyltransferase G9a modulates renal ischemia reperfusion injury by targeting Sirt1. *Free Radical Biol. Med.* **2021**, *172*, 123−135.

(35) Kellum, J. A.; Romagnani, P.; Ashuntantang, G.; Ronco, C.; Zarbock, A.; Anders, H. J. Acute kidney injury. *Nat. Rev. Dis. Primers* **2021**, *7*, No. 52.

(36) Pandey, M. K.; Gupta, S. C.; Karelia, D.; Gilhooley, P. J.; Shakibaei, M.; Aggarwal, B. B. Dietary nutraceuticals as backbone for bone health. *Biotechnol. Adv.* **2018**, *36*, 1633−1648.

(37) Thomford, N. E.; Senthebane, D. A.; Rowe, A.; Munro, D.; Seele, P.; Maroyi, A.; Dzobo, K. Natural Products for Drug Discovery in the 21st Century: Innovations for Novel Drug Discovery. *Int. J. Mol. Sci.* **2018**, *19*, No. 1578.

(38) Ruiz, S.; Pergola, P. E.; Zager, R. A.; Vaziri, N. D. Targeting the transcription factor Nrf2 to ameliorate oxidative stress and inflammation in chronic kidney disease. *Kidney Int.* **2013**, *83*, 1029−1041.

(39) Yuan, Q.; Tang, B.; Zhang, C. Signaling pathways of chronic kidney diseases, implications for therapeutics. *Signal Transduction Targeted Ther.* **2022**, *7*, No. 182.

(40) Sureshbabu, A.; Ryter, S. W.; Choi, M. E. Oxidative stress and autophagy: crucial modulators of kidney injury. *Redox Biol.* **2015**, *4*, 208−214.

(41) Diao, C. H.; Chen, Z. Y.; Qiu, T.; Liu, H.; Yang, Y. Y.; Liu, X. H.; Wu, J. F.; Wang, L. Inhibition of PRMT5 Attenuates Oxidative Stress-Induced Pyroptosis via Activation of the Nrf2/HO-1 Signal Pathway in a Mouse Model of Renal Ischemia-Reperfusion Injury. *Oxid. Med. Cell. Longevity* **2019**, *2019*, 1−18.

(42) Pergola, P. E.; Raskin, P.; Toto, R. D.; Meyer, C. J.; Huff, J. W.; Grossman, E. B.; Krauth, M.; Ruiz, S.; Audhya, P.; Christ-Schmidt, H.; Wittes, J.; Warnock, D. G. Bardoxolone methyl and kidney function in CKD with type 2 diabetes. *N. Engl. J. Med.* **2011**, *365*, 327−336.

(43) Alvarenga, L.; Salarolli, R.; Cardozo, L.; Santos, R. S.; de Brito, J. S.; Kemp, J. A.; Reis, D.; de Paiva, B. R.; Stenvinkel, P.; Lindholm, B.; Fouque, D.; Mafra, D. Impact of curcumin supplementation on expression of inflammatory transcription factors in hemodialysis patients: A pilot randomized, double-blind, controlled study. *Clin. Nutr.* **2020**, *39*, 3594−3600.

(44) Semen, K. O.; Weseler, A. R.; Janssen, M. J. W.; Drittij-Reijnders, M. J.; le Noble, J. L. M. L.; Bast, A. Effects of Monomeric and Oligomeric Flavanols on Kidney Function, Inflammation and Oxidative Stress in Runners: A Randomized Double-Blind Pilot Study. *Nutrients* **2020**, *12*, No. 1634.

(45) Medzhitov, R. Origin and physiological roles of inflammation. *Nature* **2008**, *454*, 428−435.

(46) Ren, G.; Sun, A.; Deng, C.; Zhang, J.; Wu, X.; Wei, X.; Mani, S.; Dou, W.; Wang, Z. The anti-inflammatory effect and potential mechanism of cardamonin in DSS-induced colitis. *Am. J. Physiol.: Gastrointest. Liver Physiol.* **2015**, *309*, G517−527.

(47) Sun, W.; Choi, H. S.; Kim, C. S.; Bae, E. H.; Ma, S. K.; Kim, S. W. Maslinic Acid Attenuates Ischemia/Reperfusion-Induced Acute Kidney Injury by Suppressing Inflammation and Apoptosis Through Inhibiting NF-kappaB and MAPK Signaling Pathway. *Front Pharmacol.* **2022**, *13*, No. 807452.

(48) Li, R.; Guo, Y.; Zhang, Y.; Zhang, X.; Zhu, L.; Yan, T. Salidroside Ameliorates Renal Interstitial Fibrosis by Inhibiting the TLR4/NF-kappaB and MAPK Signaling Pathways. *Int. J. Mol. Sci.* **2019**, *20*, No. 1103.

(49) Zhang, M.; Chen, Y.; Yang, M. J.; Fan, X. R.; Xie, H.; Zhang, L.; Nie, Y. S.; Yan, M. Celastrol attenuates renal injury in diabetic rats via MAPK/NF-kappaB pathway. *Phytother. Res.* **2019**, *33*, 1191−1198.

(50) Han, X.; Zhang, J.; Zhou, L.; Wei, J.; Tu, Y.; Shi, Q.; Zhang, Y.; Ren, J.; Wang, Y.; Ying, H.; Liang, G. Sclareol ameliorates hyper-

glycemia-induced renal injury through inhibiting the MAPK/NF-kappaB signaling pathway. *Phytother. Res.* **2022**, *36*, 2511−2523.

(51) Nieuwenhuijs-Moeke, G. J.; Pischke, S. E.; Berger, S. P.; Sanders, J. S. F.; Pol, R. A.; Struys, M. M. R. F.; Ploeg, R. J.; Leuvenink, H. G. D. Ischemia and Reperfusion Injury in Kidney Transplantation: Relevant Mechanisms in Injury and Repair. *J Clin. Med.* **2020**, *9*, No. 253.

(52) Chen, W.; Wang, L.; Liang, P.; Mast, J.; Mathis, C.; Liu, C. Y.; Wei, J.; Zhang, J.; Fu, L.; Juncos, L. A.; Buggs, J.; Liu, R. Reducing ischemic kidney injury through application of a synchronization modulation electric field to maintain Na(+)/K(+)-ATPase functions. *Sci. Transl. Med.* **2022**, *14*, No. eabj4906.

(53) Yan, J.; Wang, Y.; Zhang, J.; Liu, X.; Yu, L.; He, Z. Rapidly Blocking the Calcium Overload/ROS Production Feedback Loop to Alleviate Acute Kidney Injury via Microenvironment-Responsive BAPTA-AM/BAC Co-Delivery Nanosystem. *Small* **2023**, *19*, No. 2206936.

(54) Collett, J. A.; Mehrotra, P.; Crone, A.; Shelley, W. C.; Yoder, M. C.; Basile, D. P. Endothelial colony-forming cells ameliorate endothelial dysfunction via secreted factors following ischemia-reperfusion injury. *Am. J. Physiol.: Renal Physiol.* **2017**, *312*, F897−F907.